Supplementary Information

Discovery of new 1,3-diphenylurea appended aryl pyridine derivatives as apoptosis inducers through c-MET and VEGFR-2 inhibition: Design, synthesis, *in vivo* and *in silico* studies

Heba A. Elsebaie[1,†], **Mohamed S. Nafie**[2,3,†], **Haytham O. Tawfik**[1,4,*], **Amany Belal**[5], **Mohammed M. Ghoneim**[6], **Ahmad J. Obaidullah**[7], **Salwa Shaaban**[8,9], **Abdelmoneim A. Ayed**[10], **Mohamed El-Naggar**[11], **Ahmed B. M. Mehany**[12], **Moataz A. Shaldam**[13,4,*]

[1] *Department of Pharmaceutical Chemistry, Faculty of Pharmacy, Tanta University, Tanta 31527, Egypt.*
[2] *Department of Chemistry, College of Sciences, University of Sharjah, Sharjah 27272, United Arab Emirates (UAE).*
[3] *Chemistry Department, Faculty of Science, Suez Canal University, Ismailia 41522, Egypt.*
[4] *Department of Pharmaceutical Chemistry, Faculty of Pharmacy, AlSalam University in Egypt, Kafr Al Zaiyat, 6615062, Egypt.*
[5] *Department of Pharmaceutical Chemistry, College of Pharmacy, Taif University, P.O. Box 11099, Taif 21944, Saudi Arabia.*
[6] *Department of Pharmacy Practice, College of Pharmacy, AlMaarefa University, Ad Diriyah, Riyadh 13713, Saudi Arabia.*
[7] *Department of Pharmaceutical Chemistry, College of Pharmacy, King Saud University, P.O. Box 2457, Riyadh 11451, Saudi Arabia*
[8] *Department of Microbiology & Immunology, Faculty of pharmacySuef University, Beni-Suef, Egypt.*
[9] *Department of Clinical Laboratory Sciences, Faculty of Applied medical Sciences, King Khalid University, Abha, Saudi Arabia.*
[10] *Department of Chemistry, Faculty of Science, Cairo University, Giza, Cairo 12613, Egypt.*
[11] *Chemistry department, Faculty of Sciences, Pure and Applied Chemistry Group, University of Sharjah, P. O. Box 27272, Sharjah, United Arab Emirates*
[12] *Zoology Department, Faculty of Science (Boys), Al-Azhar University, Cairo 11884, Egypt.*
[13] *Department of Pharmaceutical Chemistry, Faculty of Pharmacy, Kafrelsheikh University, Kafrelsheikh, P.O. Box 33516, Egypt.*

[†] Equally contributed.

* H. O. Tawfik; haytham.omar.mahmoud@pharm.tanta.edu.eg

* M. A. Shaldam; dr_moutaz_986@pharm.kfs.edu.eg

Table of Contents

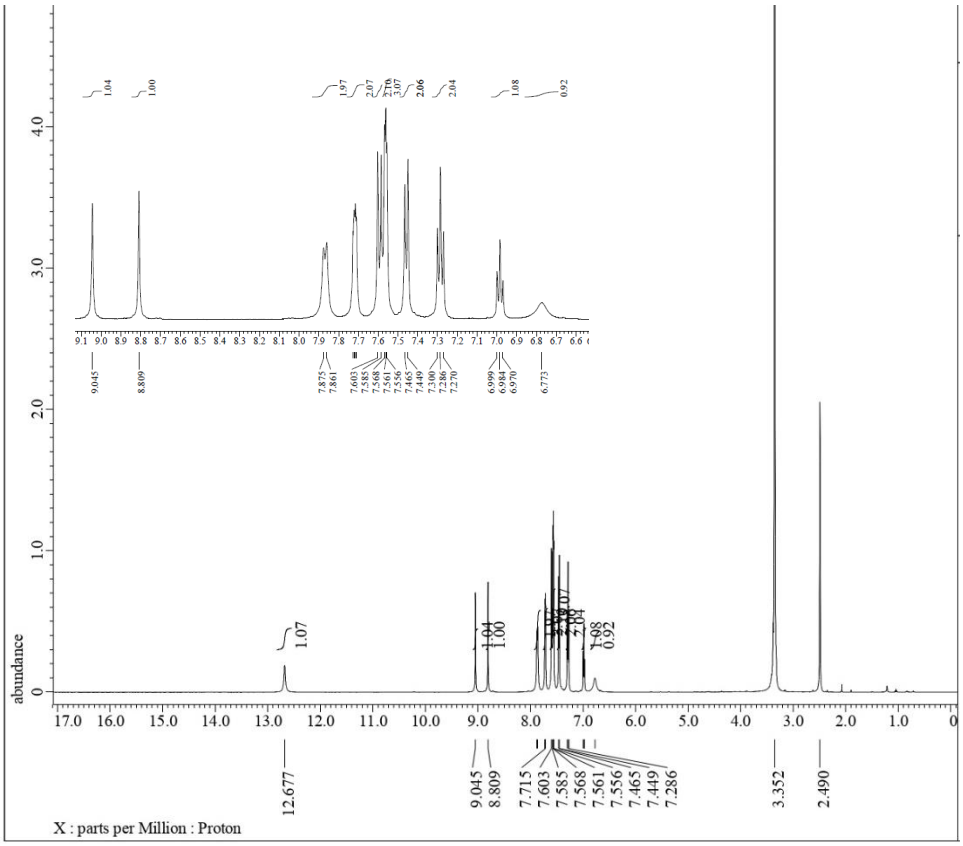

Figure S1. ^{1}H NMR (500 MHz, DMSO-d_6) spectrum of compound **2a**

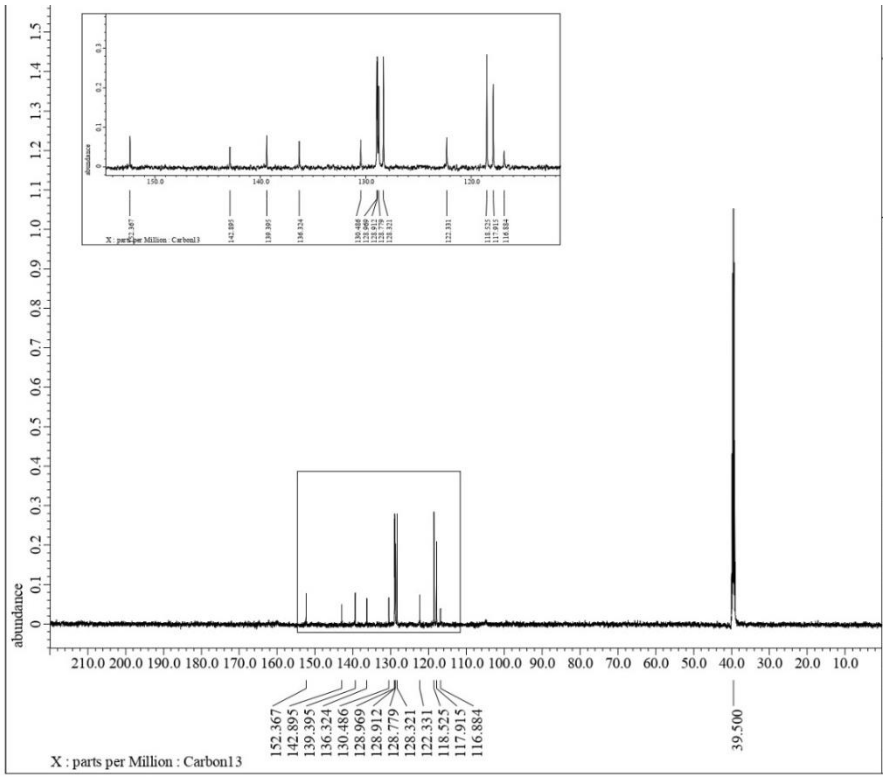

Figure S2. ^{13}C NMR (125 MHz, DMSO-d_6) spectrum of compound **2a**

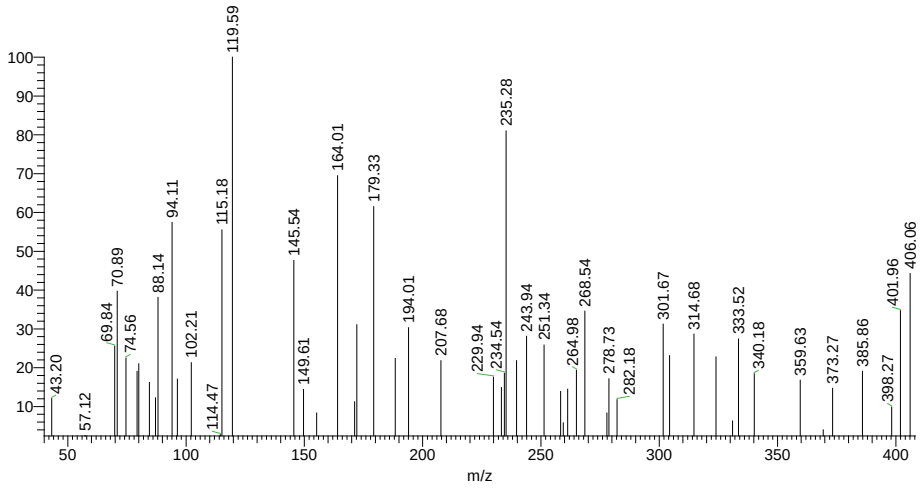

Figure S3. Mass spectrum of compound **2a**

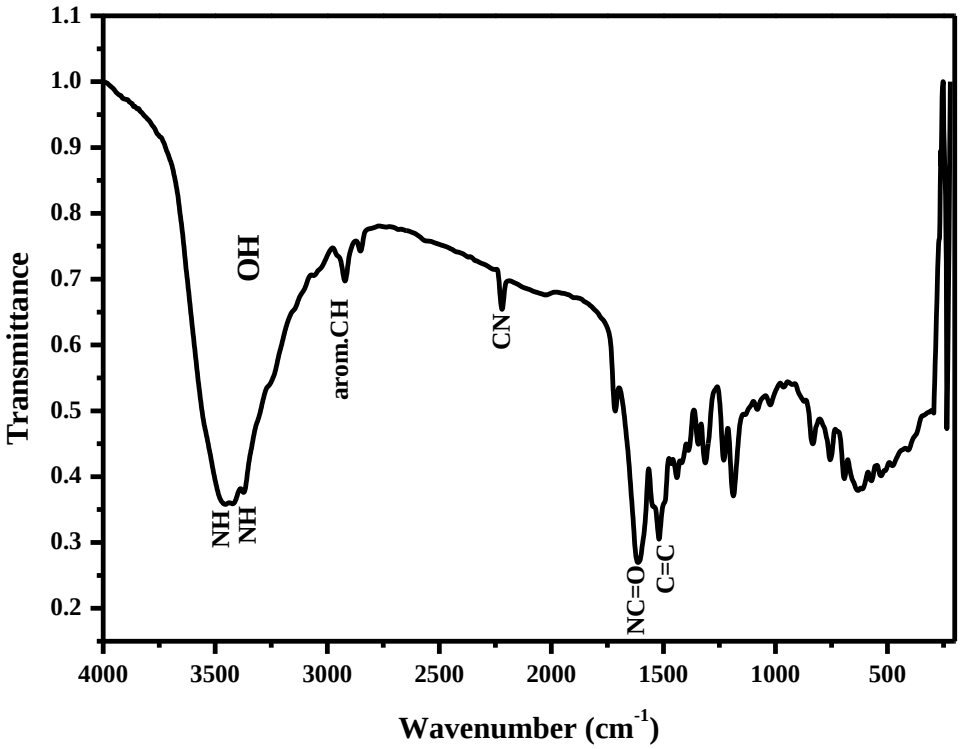

Figure S4. IR spectrum of compound **2a**

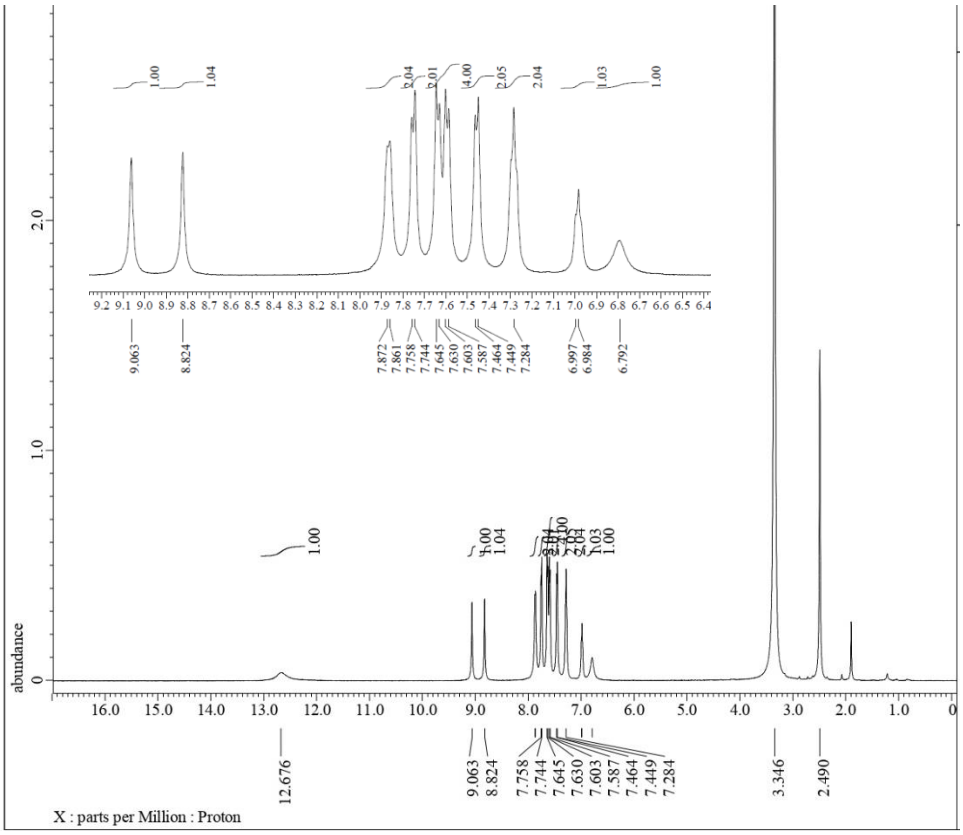

Figure S5. ^{1}H NMR (500 MHz, DMSO-d_6) spectrum of compound **2b**

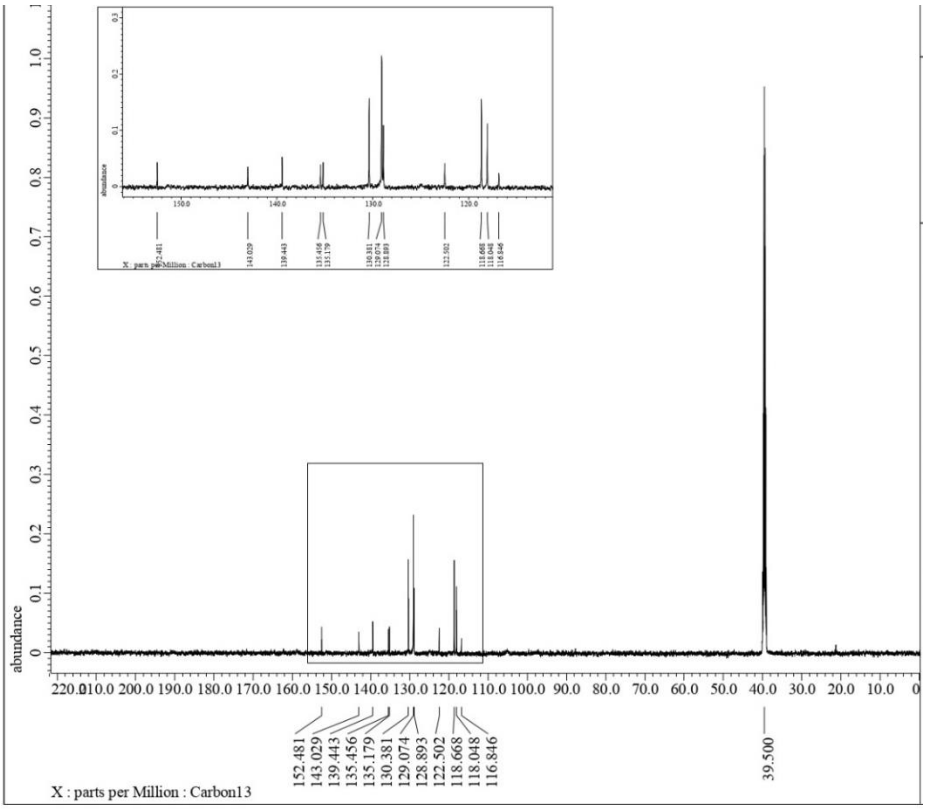

Figure S6. ^{13}C NMR (125 MHz, DMSO-d_6) spectrum of compound **2b**

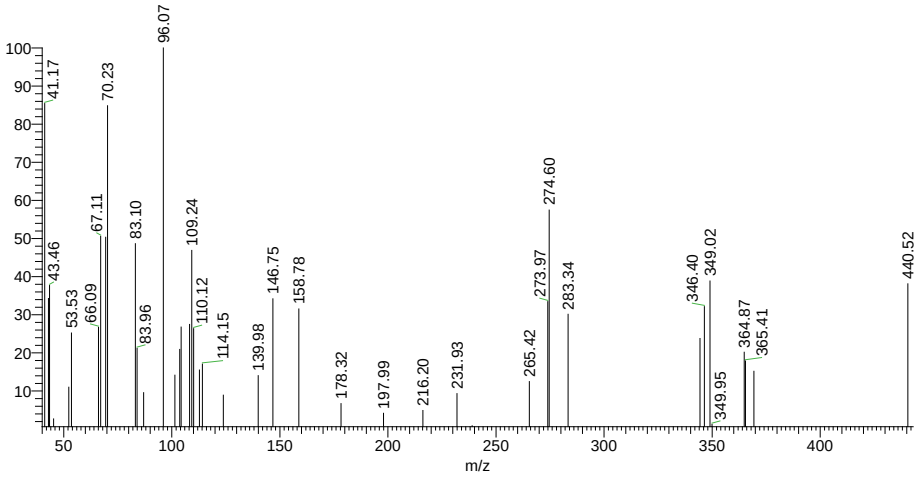

Figure S7. Mass spectrum of compound **2b**

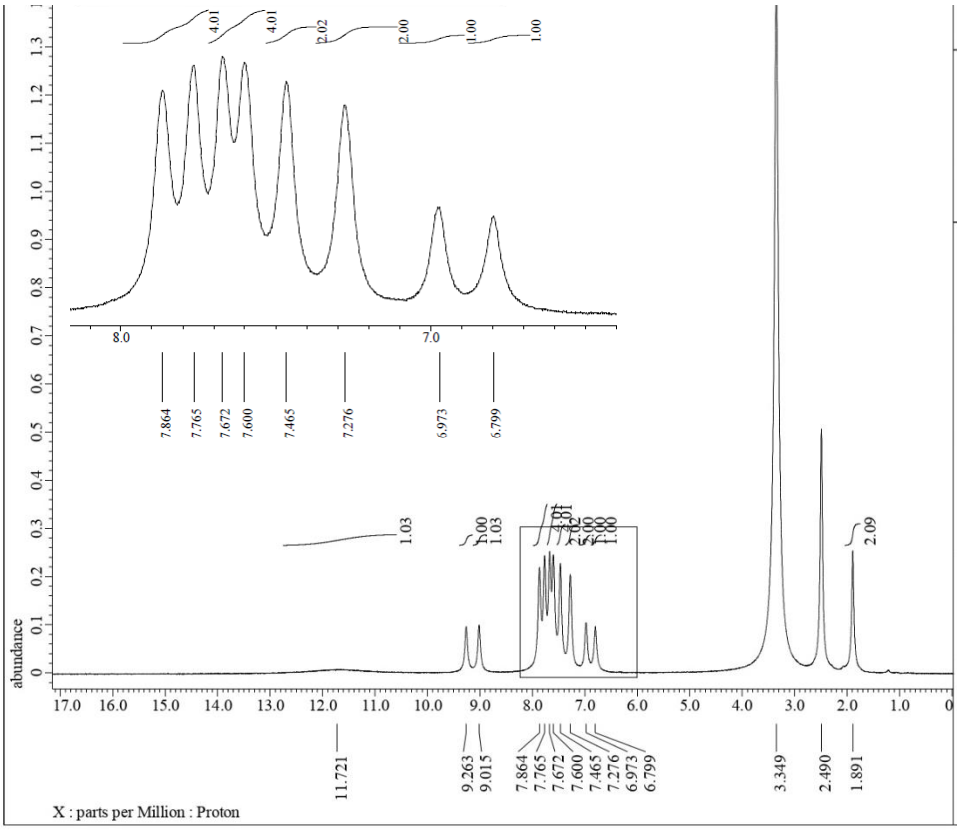

Figure S8. ^{1}H NMR (500 MHz, DMSO-d_6) spectrum of compound **2c**

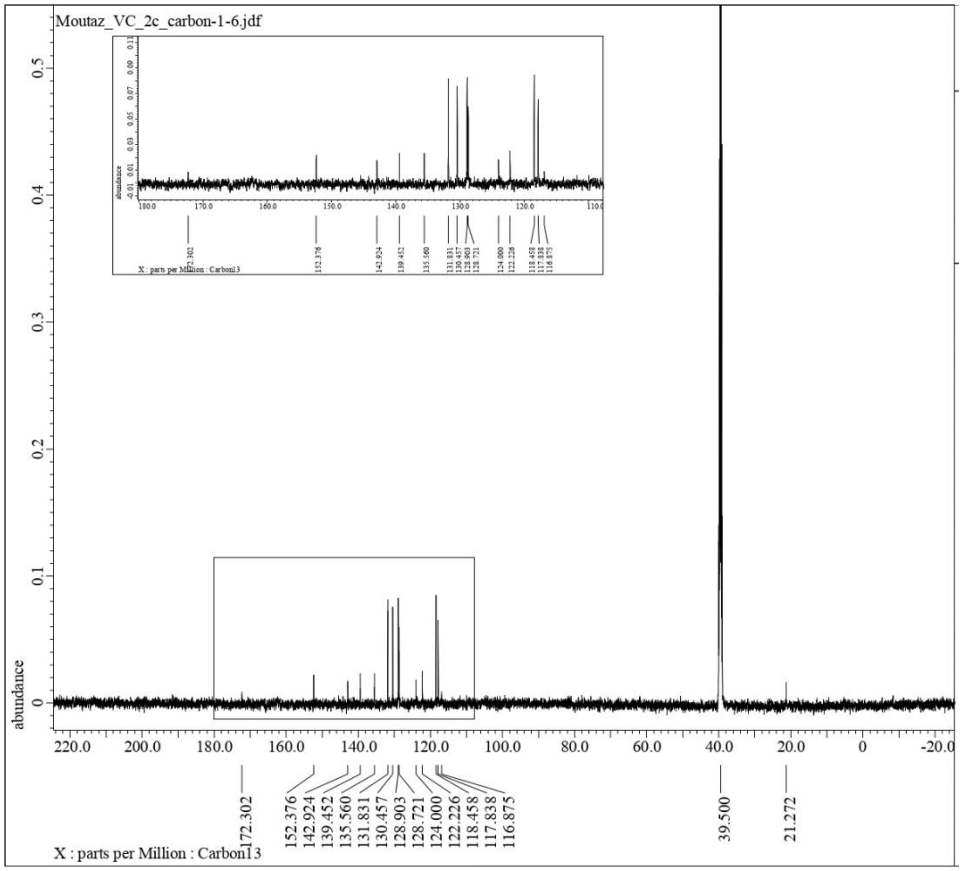

Figure S9. ^{13}C NMR (125 MHz, DMSO-d_6) spectrum of compound **2c**

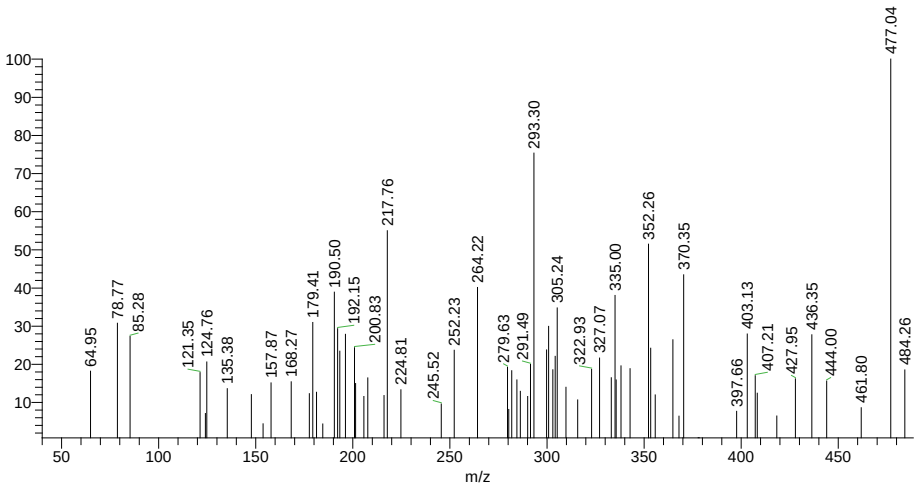

Figure S10. Mass spectrum of compound **2c**

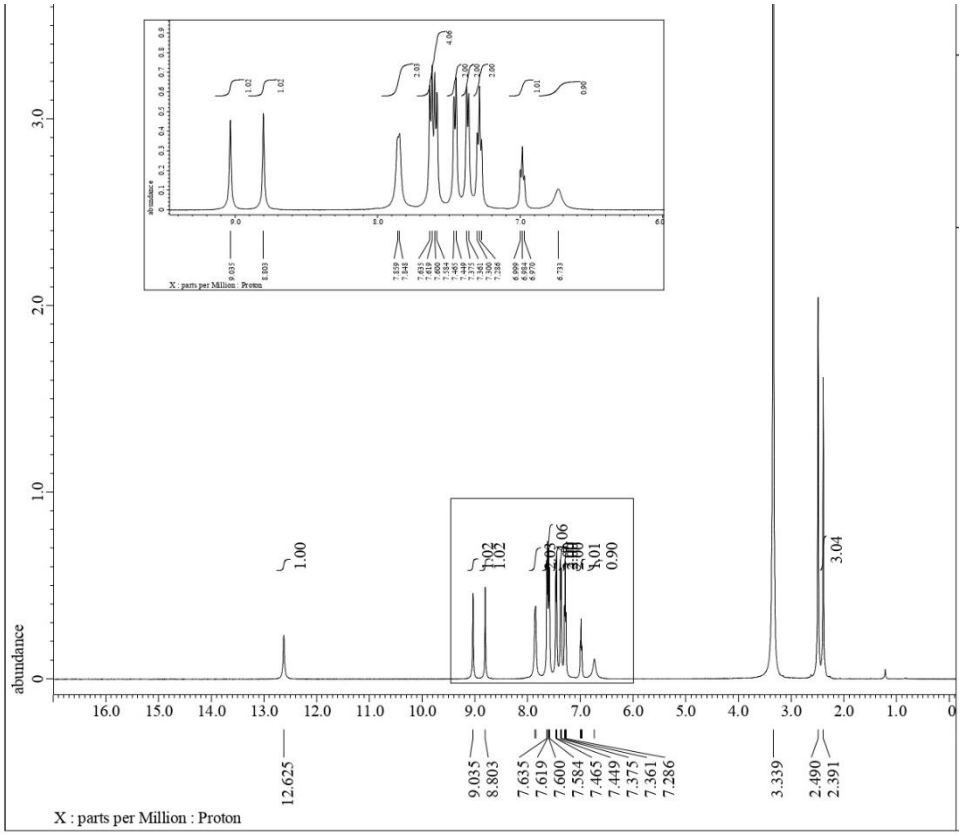

Figure S11. ^{1}H NMR (500 MHz, DMSO-d_6) spectrum of compound **2d**

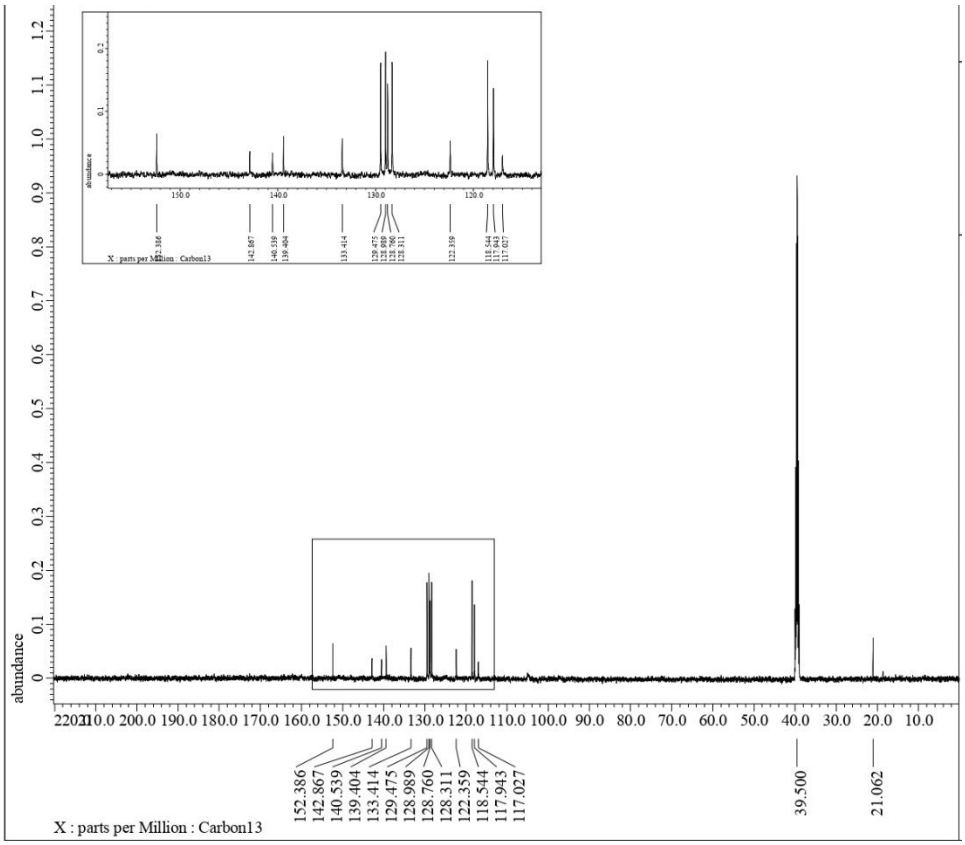

Figure S12. ^{13}C NMR (125 MHz, DMSO-d_6) spectrum of compound **2d**

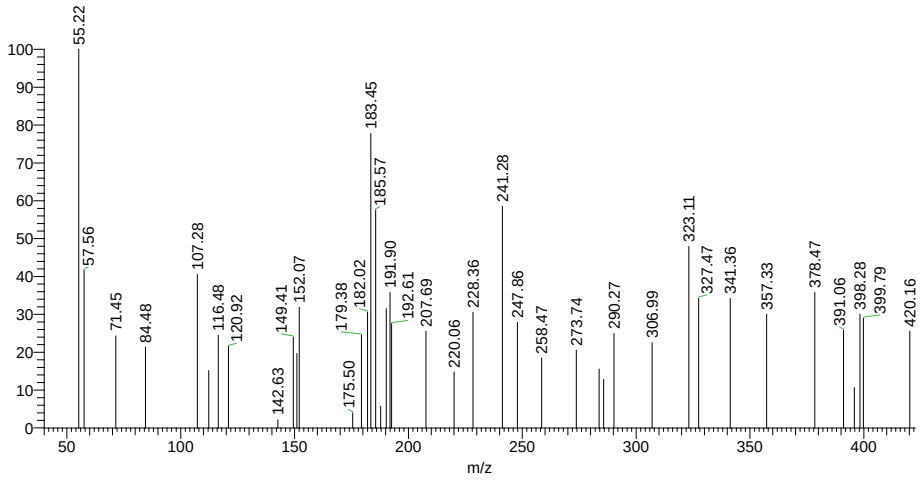

Figure S13. Mass spectrum of compound **2d**

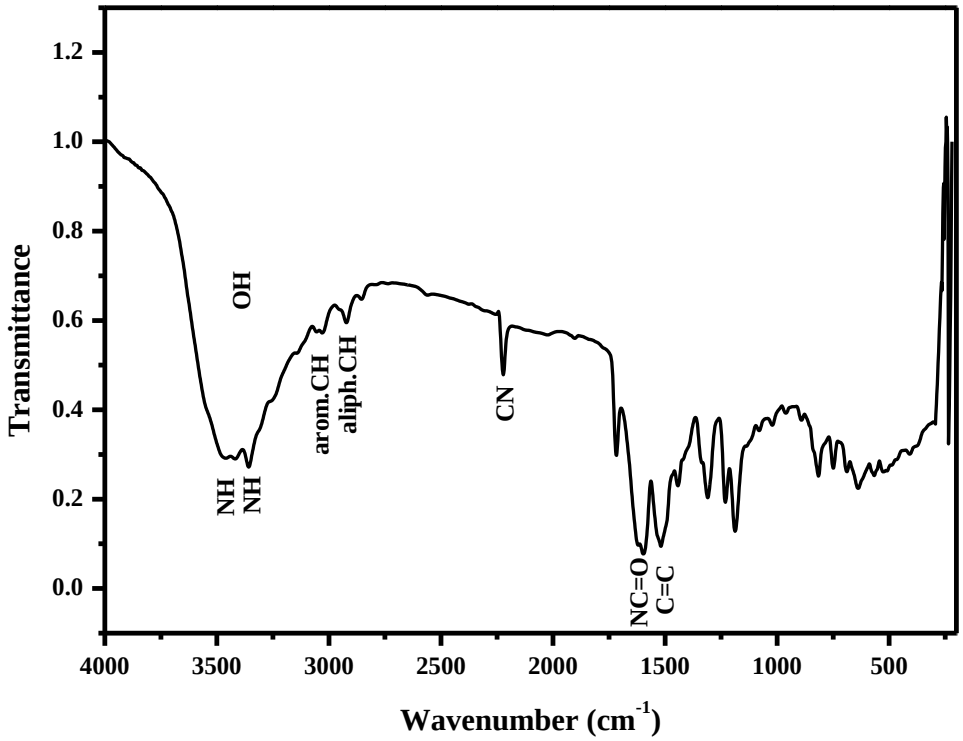

Figure S14. IR spectrum of compound **2d**

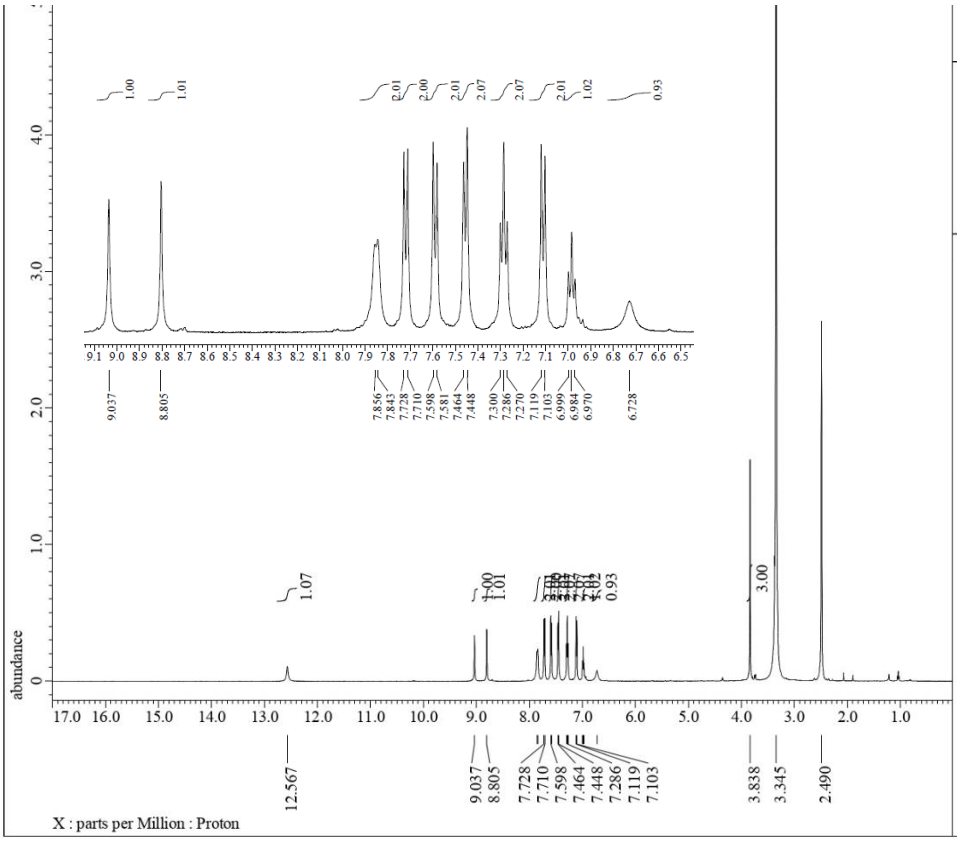

Figure S15. ^{1}H NMR (500 MHz, DMSO-d_6) spectrum of compound **2e**

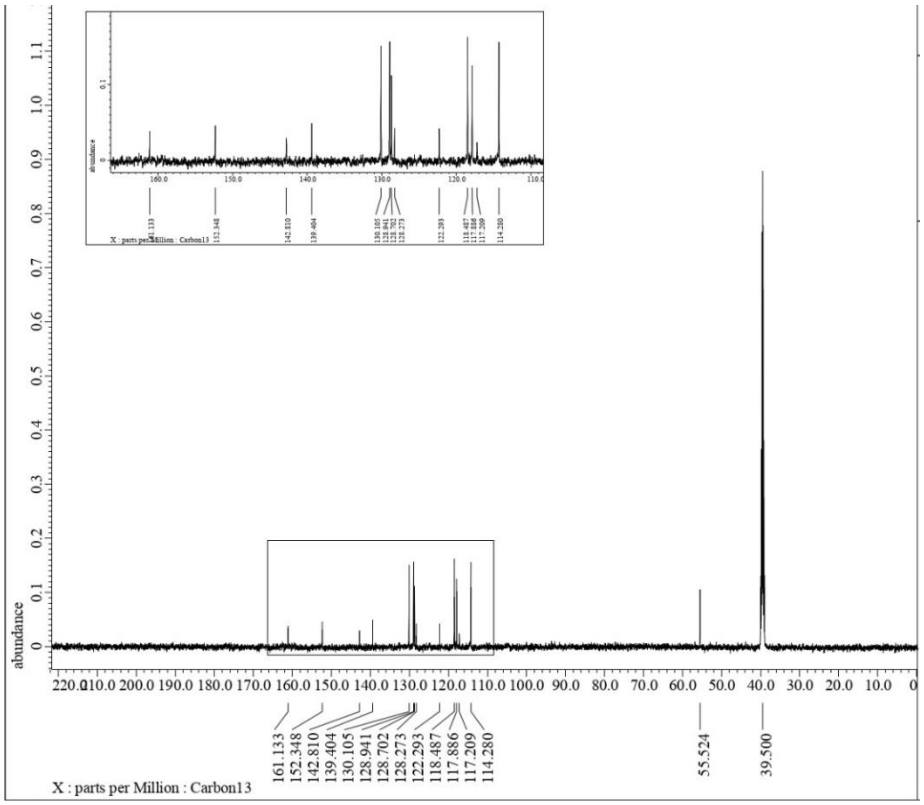

Figure S16. ^{13}C NMR (125 MHz, DMSO-d_6) spectrum of compound **2e**

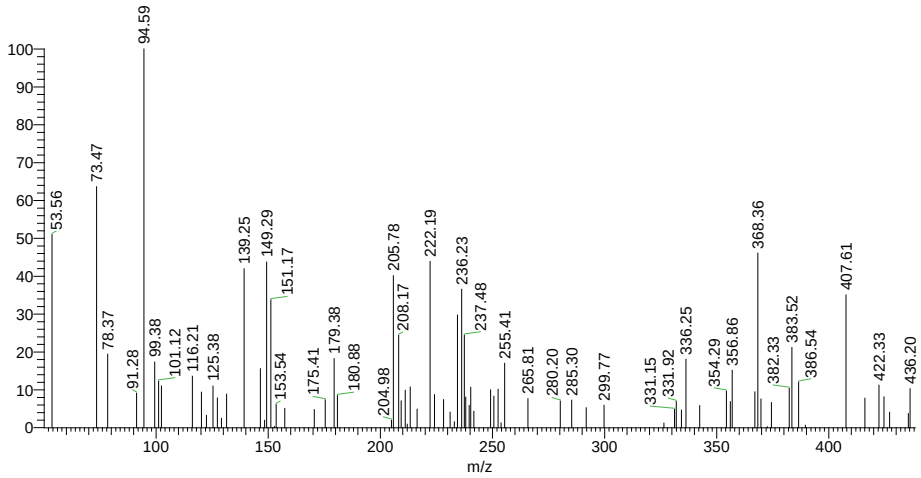

Figure S17. Mass spectrum of compound **2e**

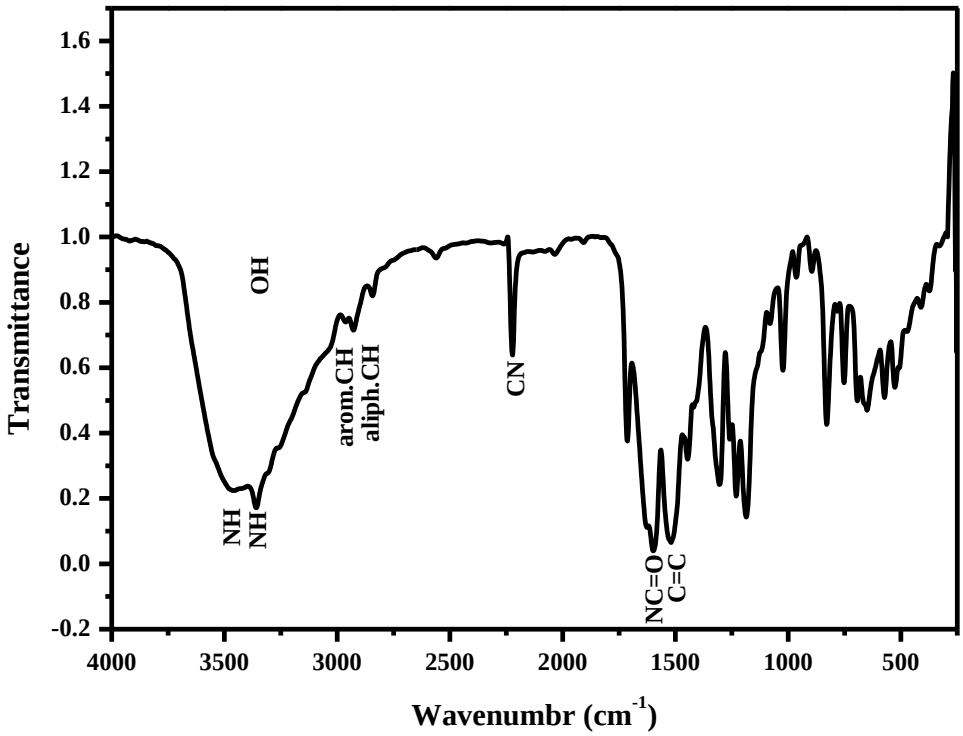

Figure S18. IR spectrum of compound **2e**

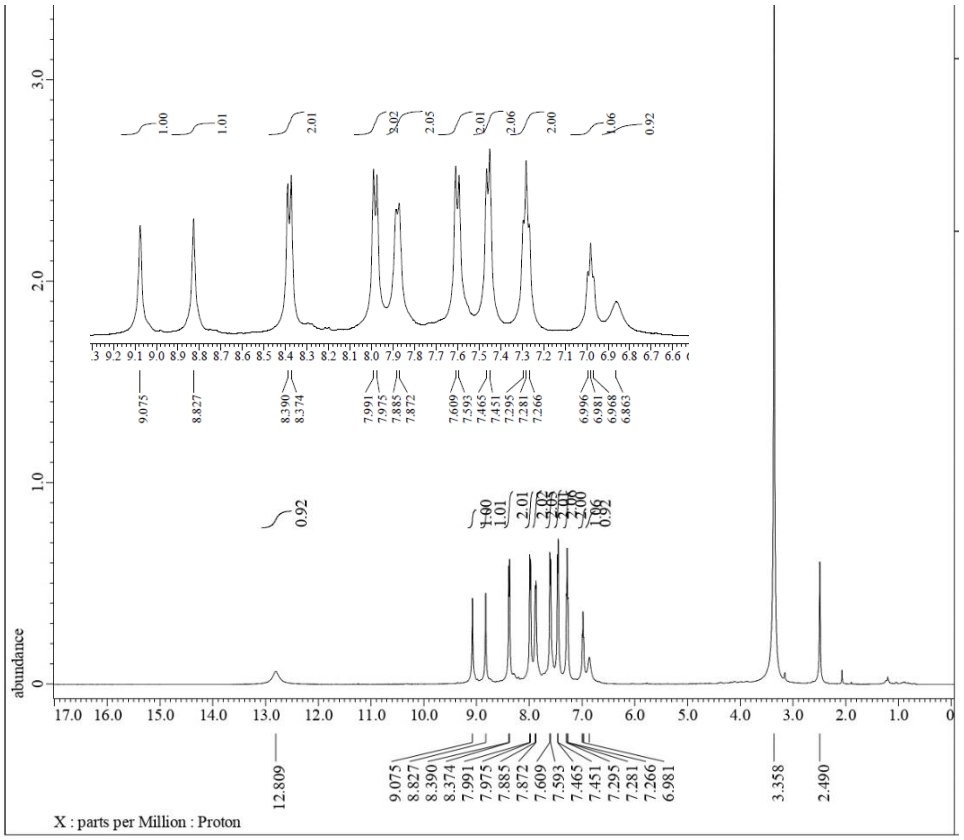

Figure S19. ^{1}H NMR (500 MHz, DMSO-d_6) spectrum of compound **2f**

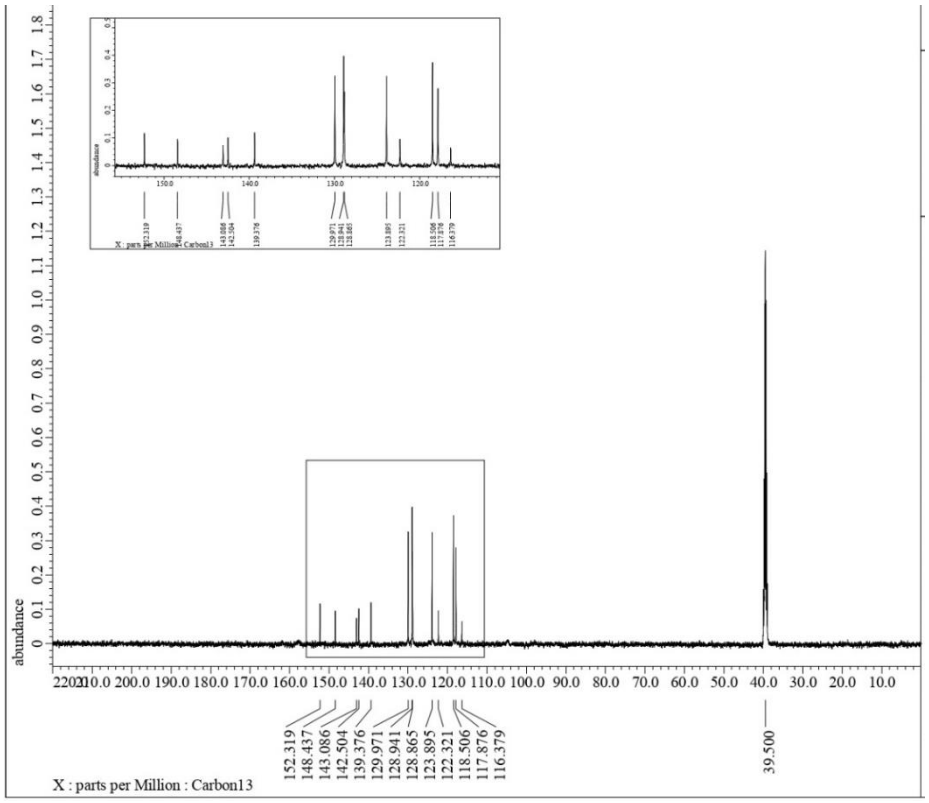

Figure S20. ^{13}C NMR (125 MHz, DMSO-d_6) spectrum of compound **2f**

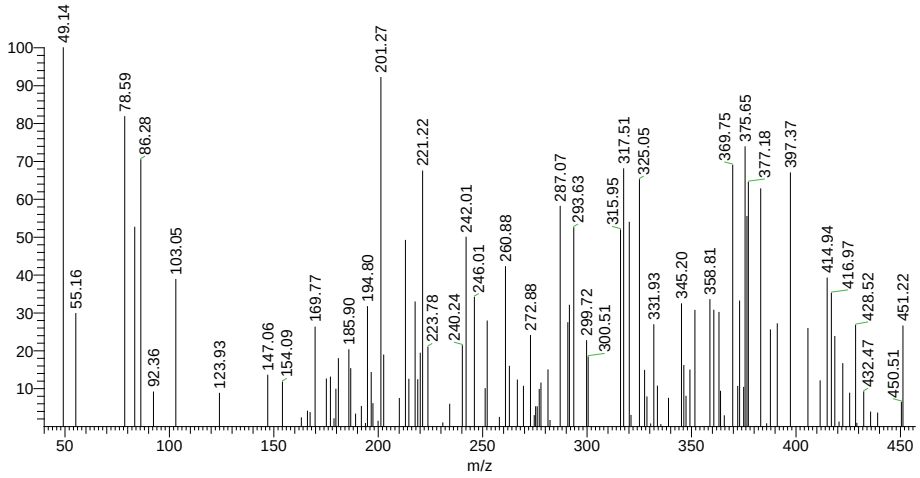

Figure S21. Mass spectrum of compound **2f**

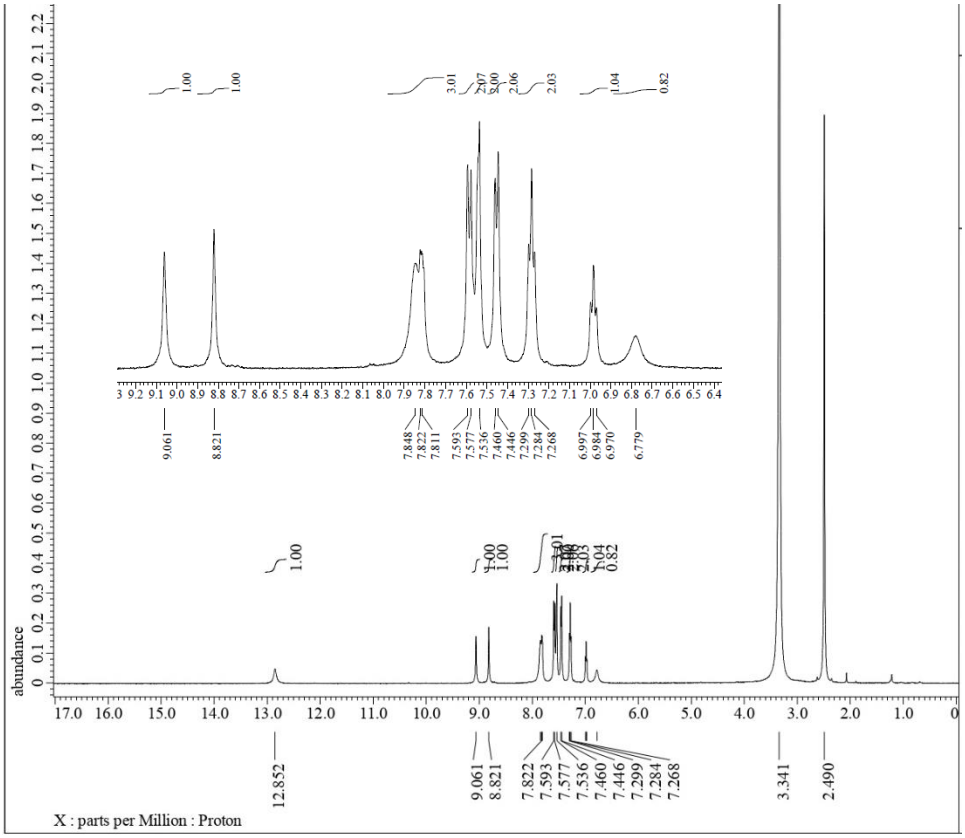

Figure S22. ^{1}H NMR (500 MHz, DMSO-d_6) spectrum of compound **2g**

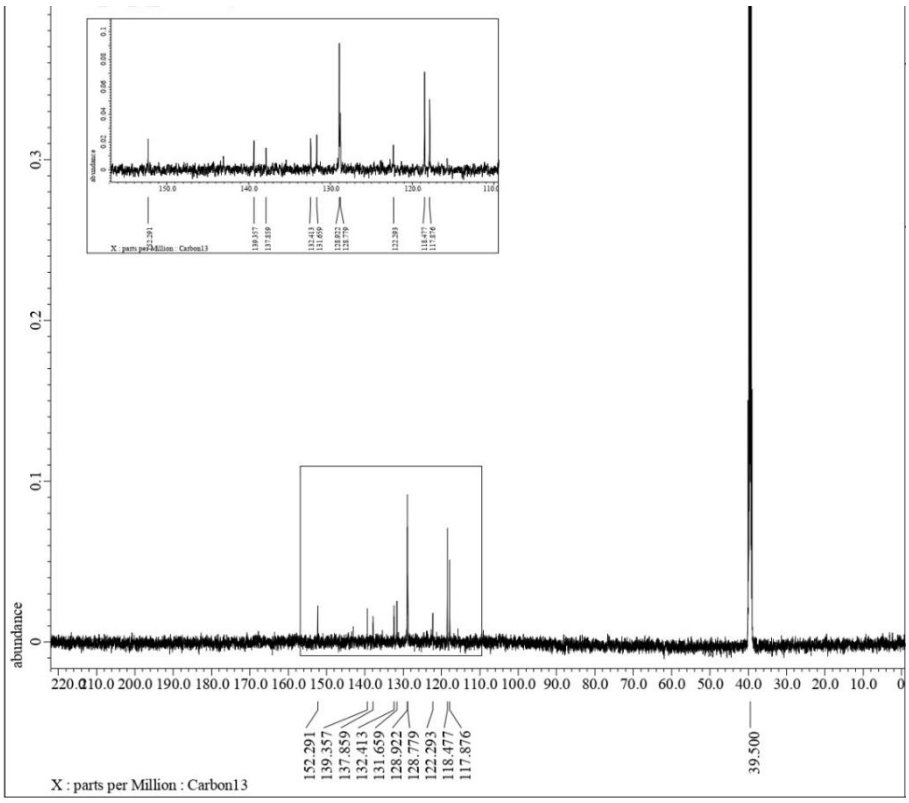

Figure S23. ^{13}C NMR (125 MHz, DMSO-d_6) spectrum of compound **2g**

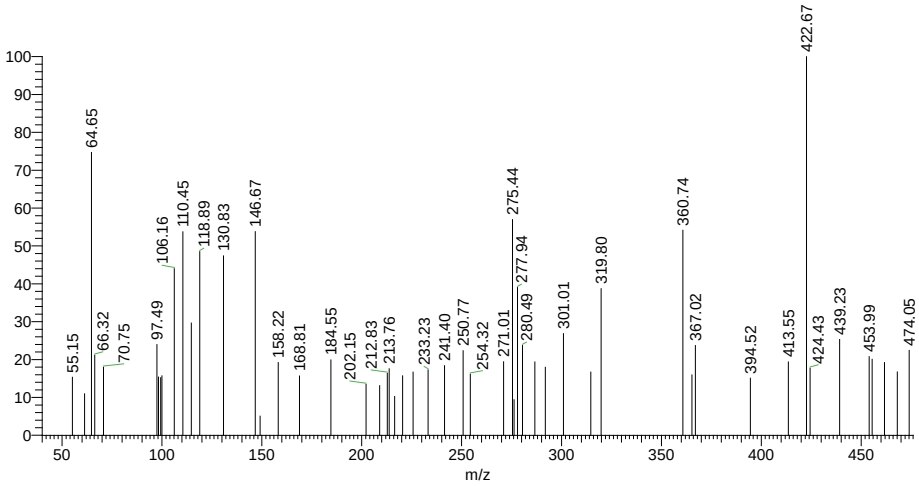

Figure S24. Mass spectrum of compound **2g**

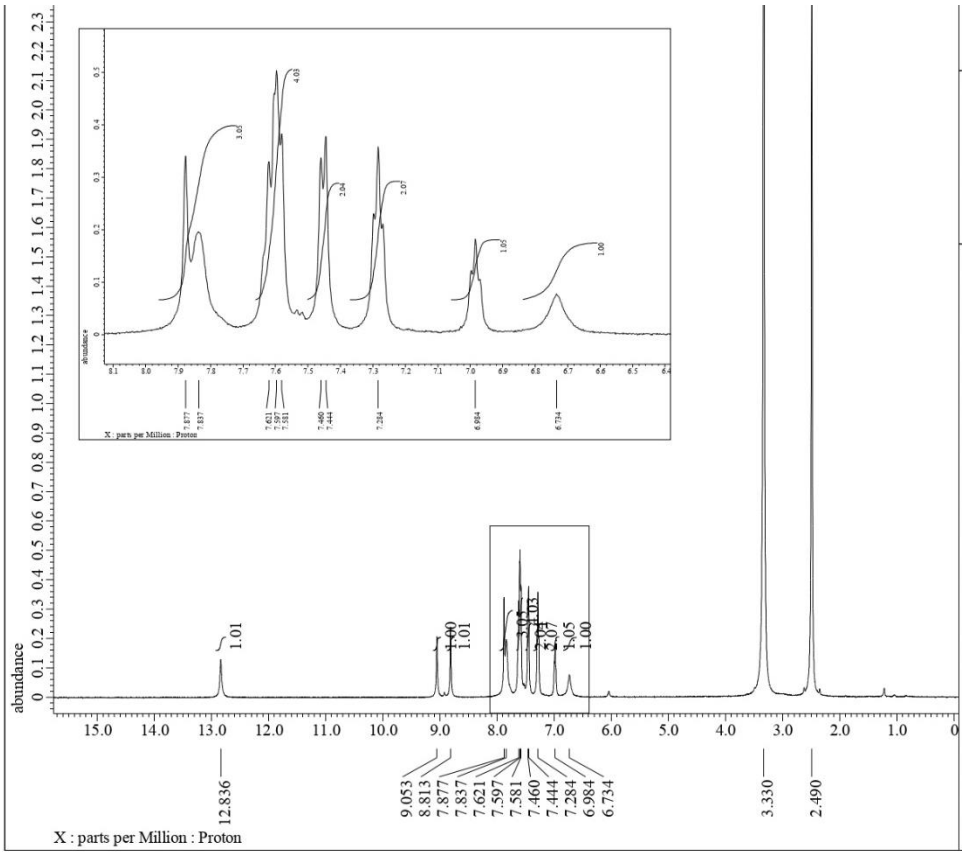

Figure S25. ^{1}H NMR (500 MHz, DMSO-d_6) spectrum of compound **2h**

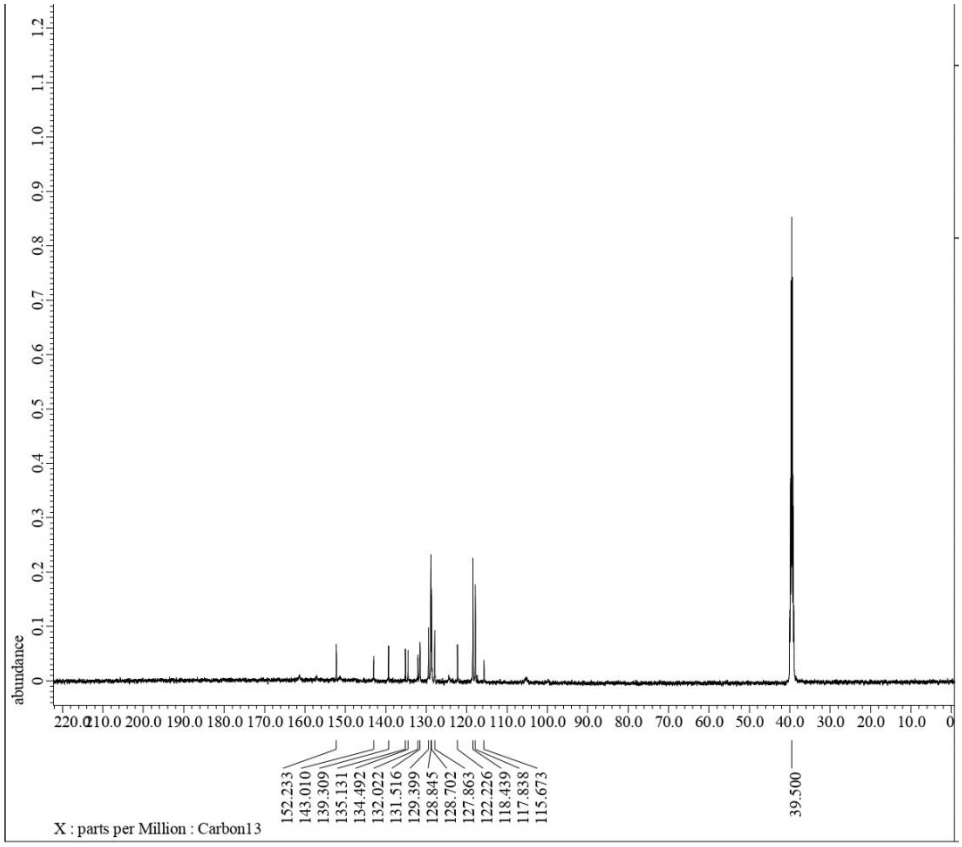

Figure S26. ^{13}C NMR (125 MHz, DMSO-d_6) spectrum of compound **2h**

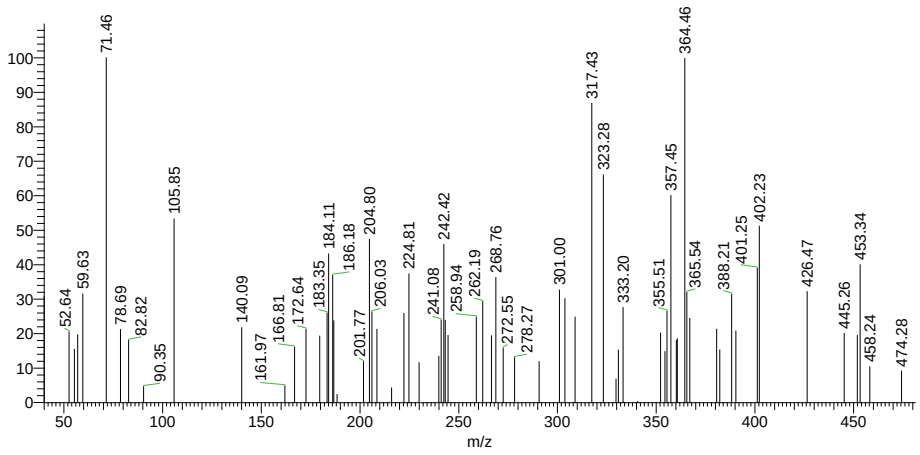

Figure S27. Mass spectrum of compound **2h**

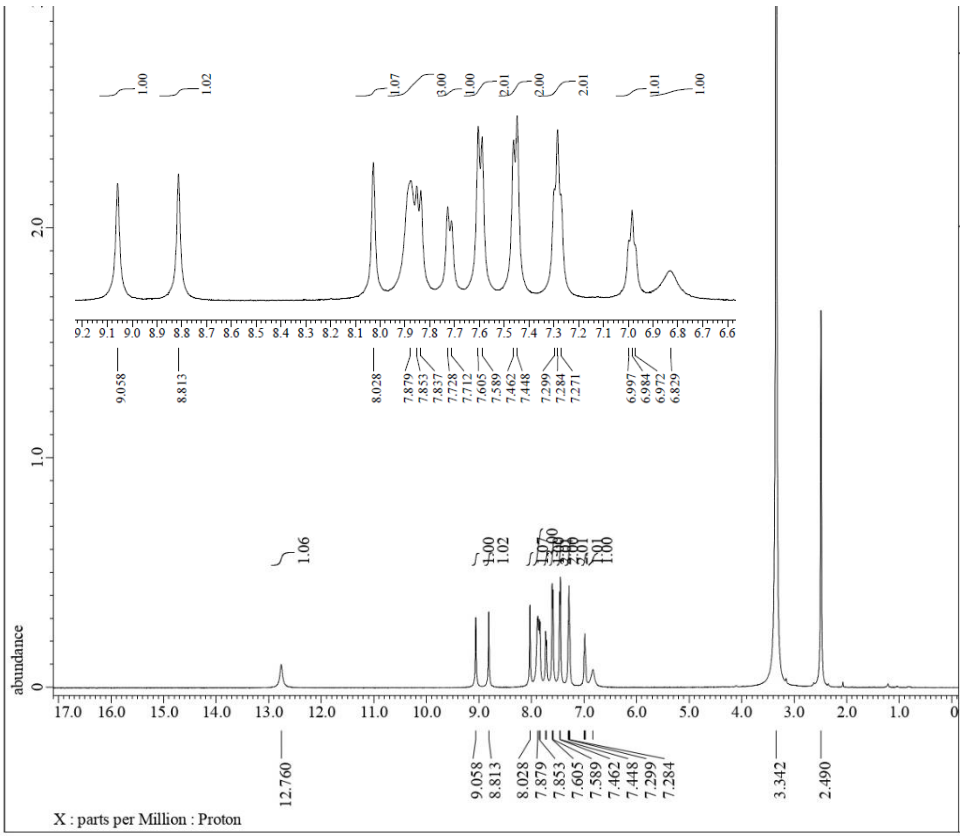

Figure S28. ^{1}H NMR (500 MHz, DMSO-d_6) spectrum of compound **2i**

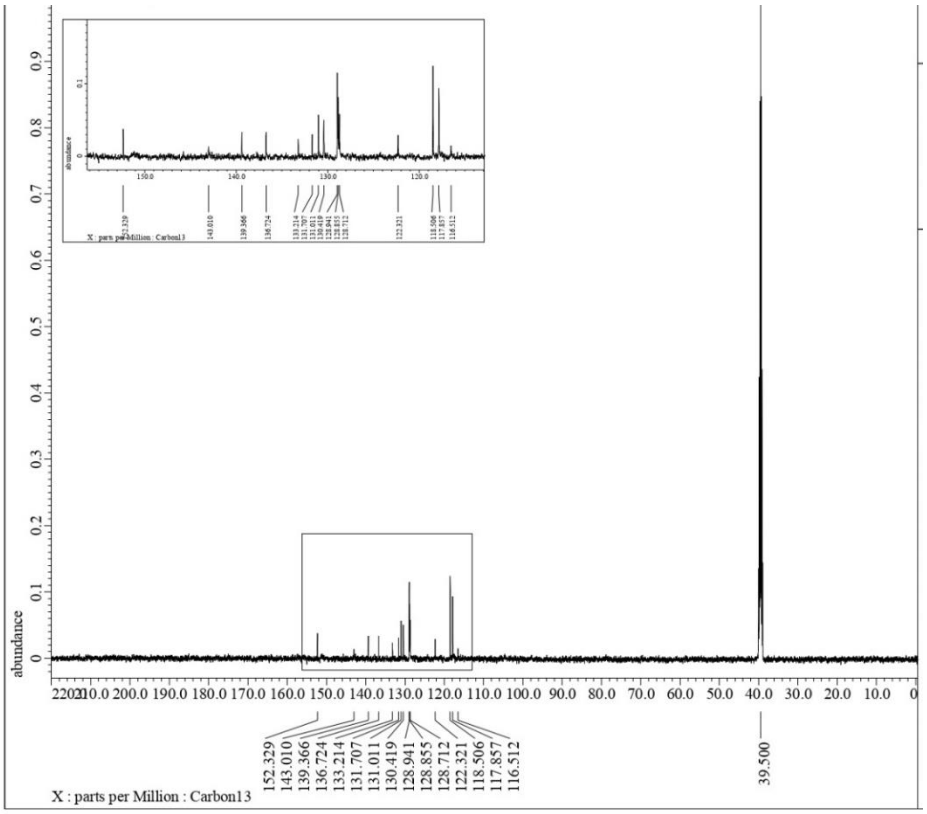

Figure S29. ^{13}C NMR (125 MHz, DMSO-d_6) spectrum of compound **2i**

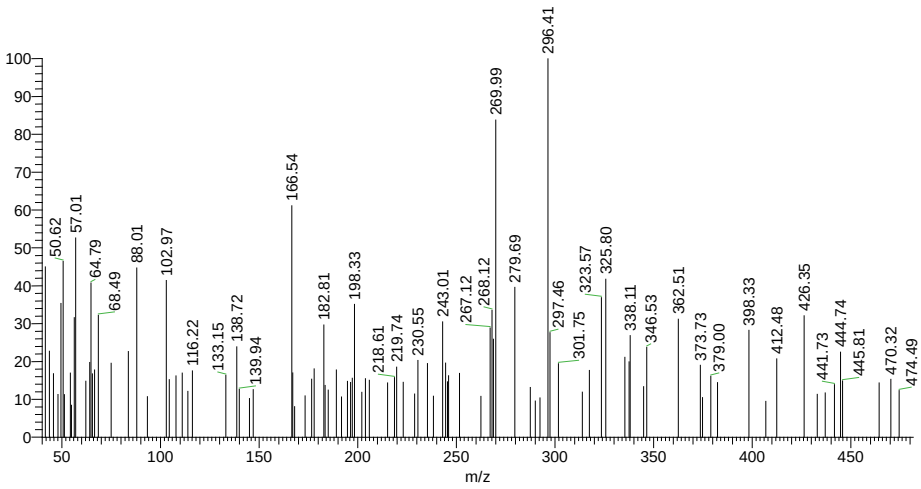

Figure S30. Mass spectrum of compound **2i**

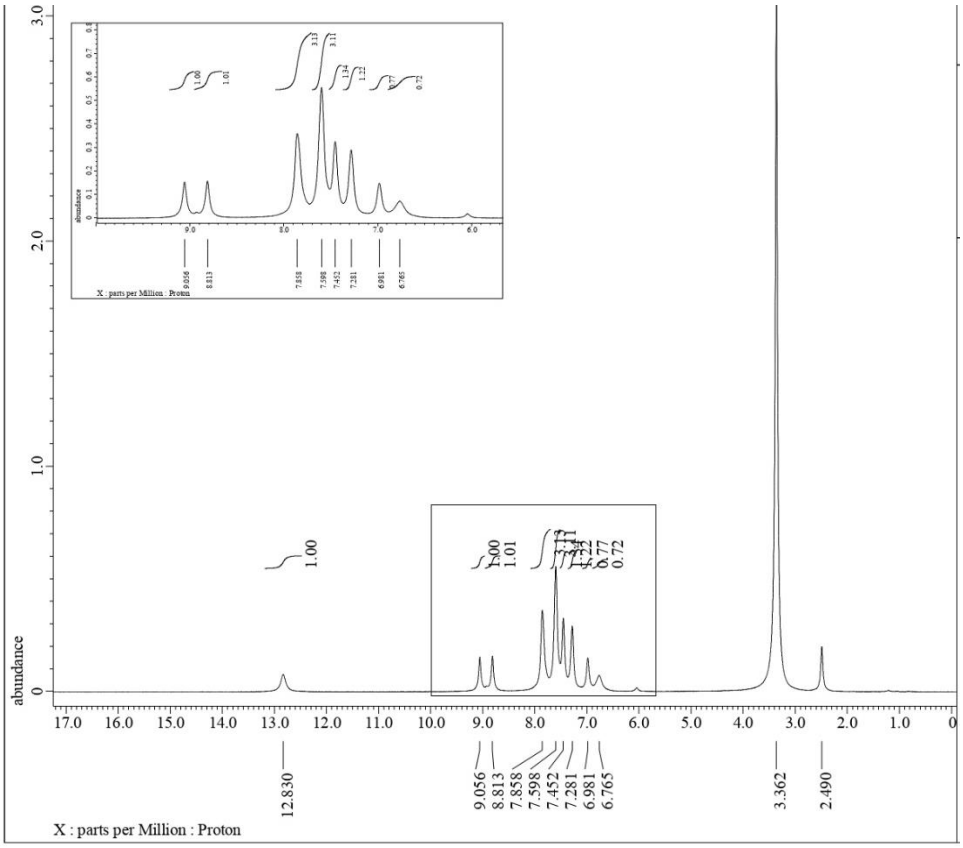

Figure S31. ^{1}H NMR (500 MHz, DMSO-d_6) spectrum of compound **2j**

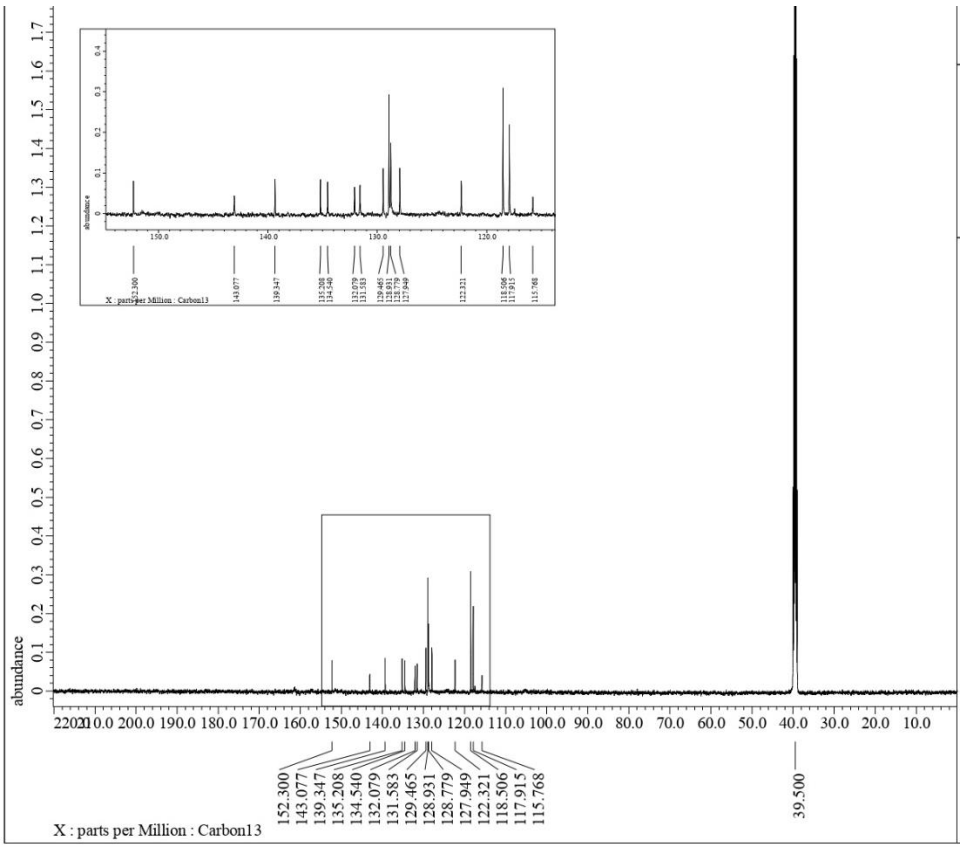

Figure S32. ^{13}C NMR (125 MHz, DMSO-d_6) spectrum of compound **2j**

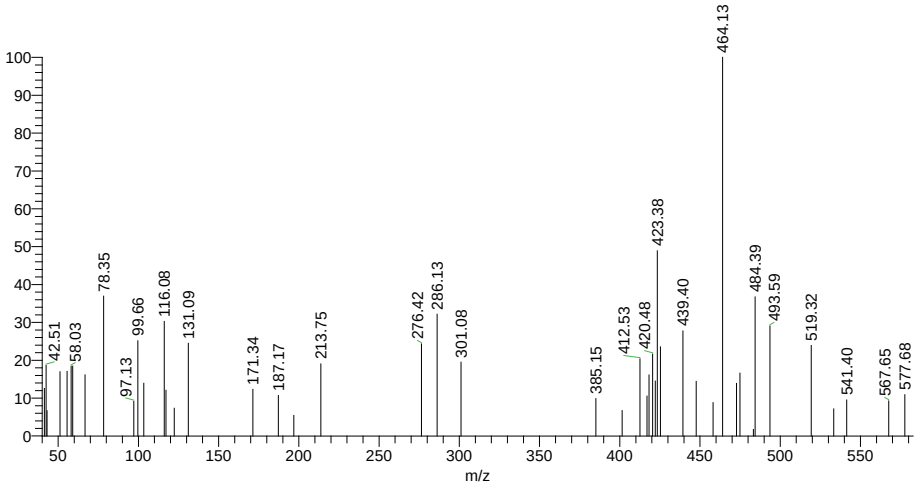

Figure S33. Mass spectrum of compound **2j**

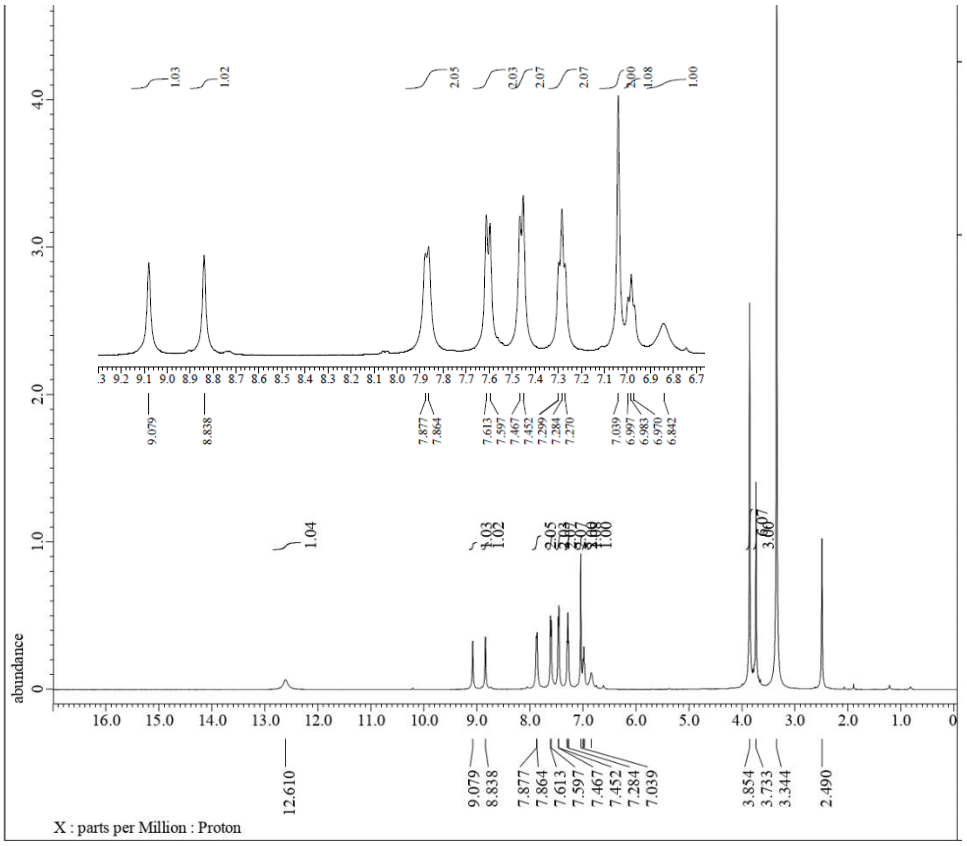

Figure S34. ^{1}H NMR (500 MHz, DMSO-d_6) spectrum of compound **2k**

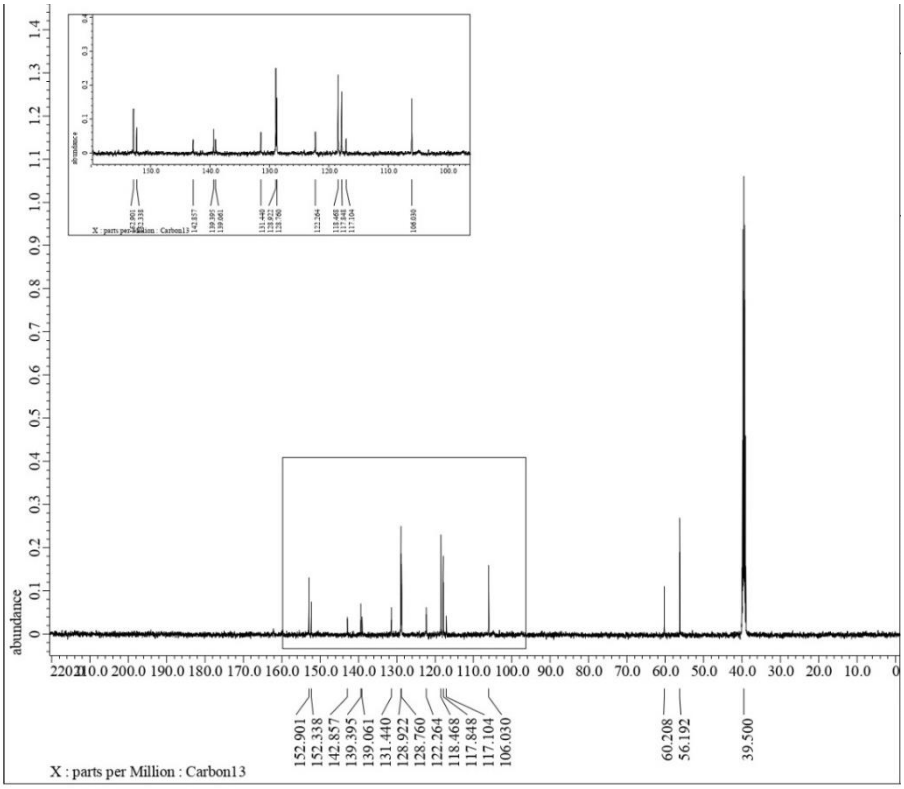

Figure S35. ^{13}C NMR (125 MHz, DMSO-d_6) spectrum of compound **2k**

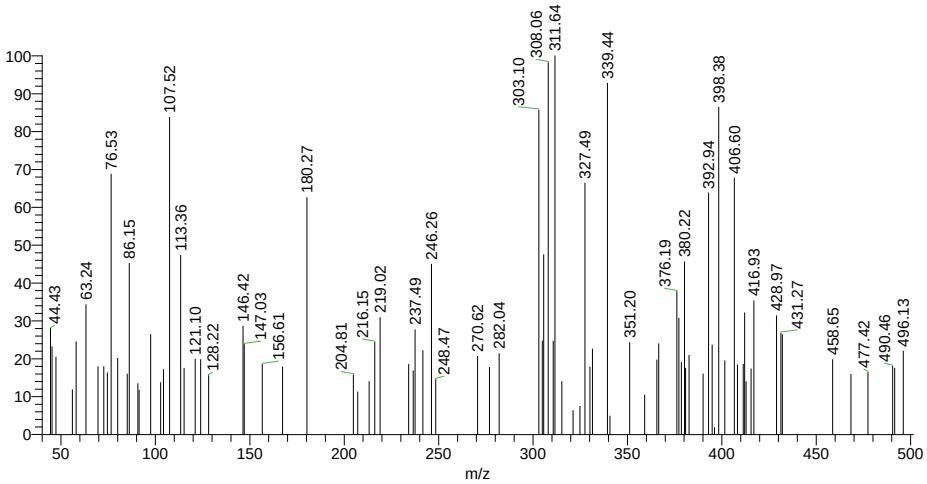

Figure S36. Mass spectrum of compound **2k**

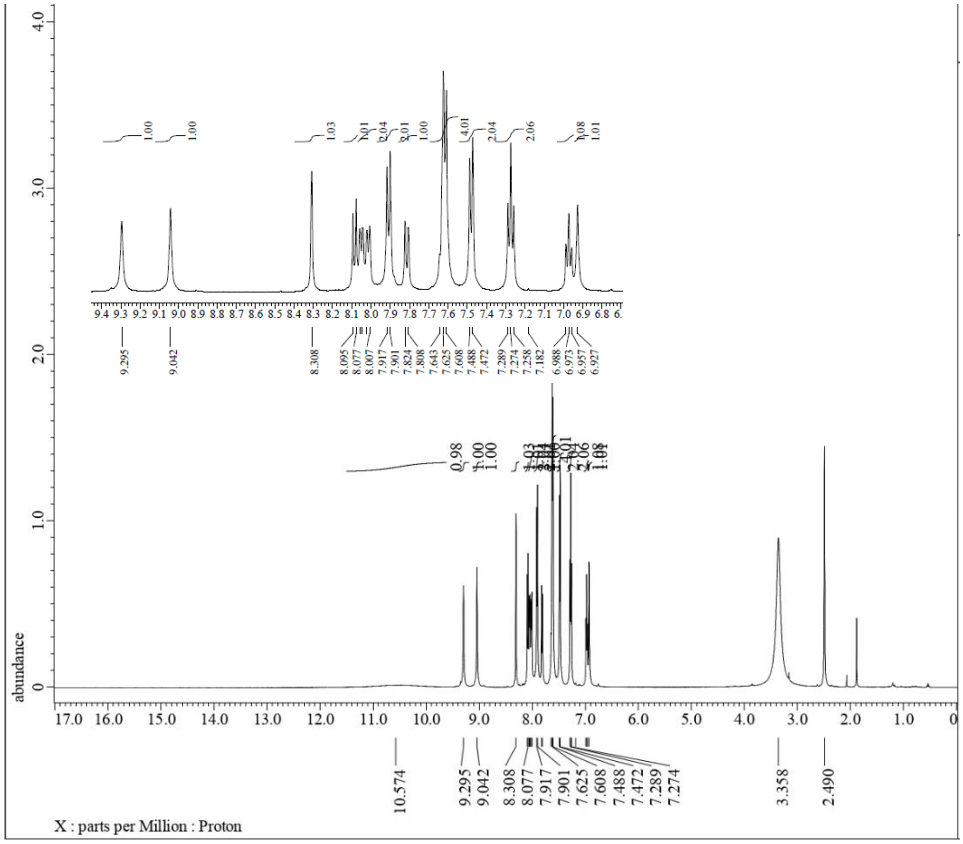

Figure S37. ^{1}H NMR (500 MHz, DMSO-d_6) spectrum of compound **2l**

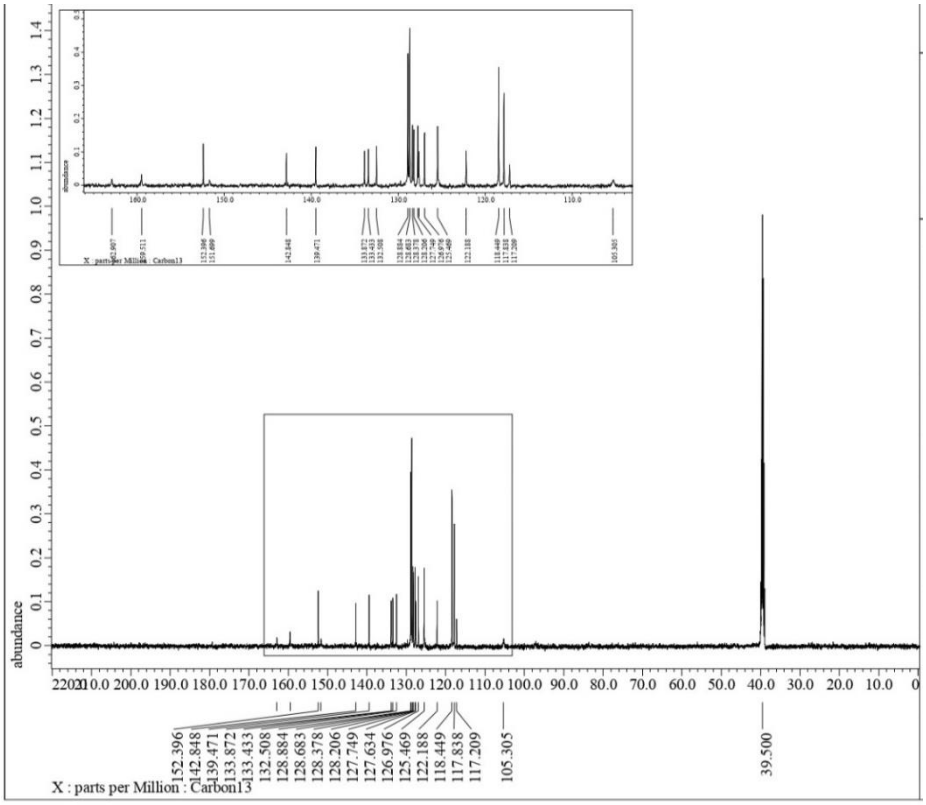

Figure S38. ^{13}C NMR (125 MHz, DMSO-d_6) spectrum of compound **2l**

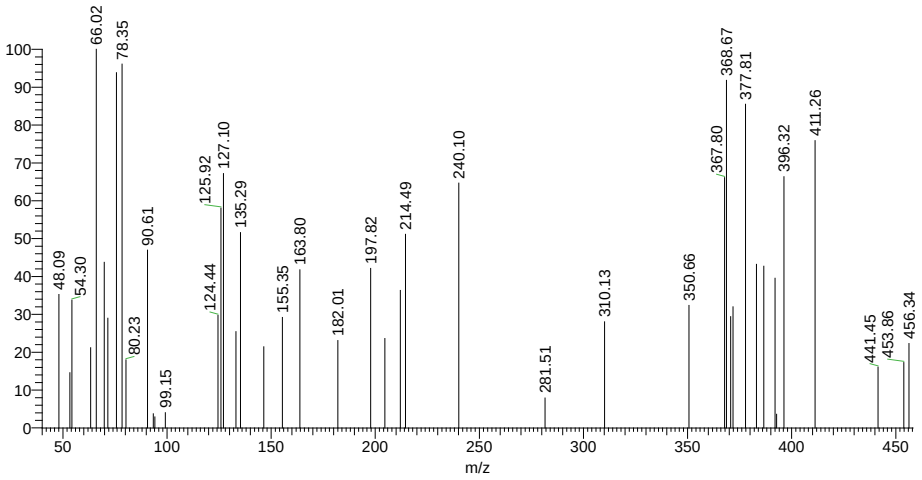

Figure S39. Mass spectrum of compound **2l**

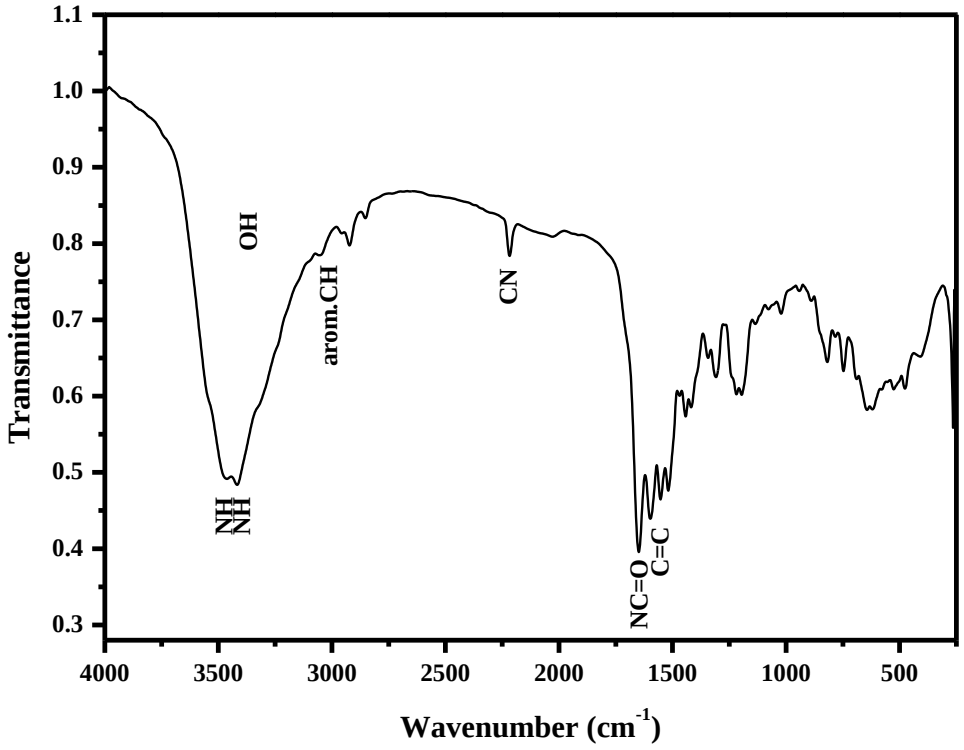

Figure S40. IR spectrum of compound **2l**

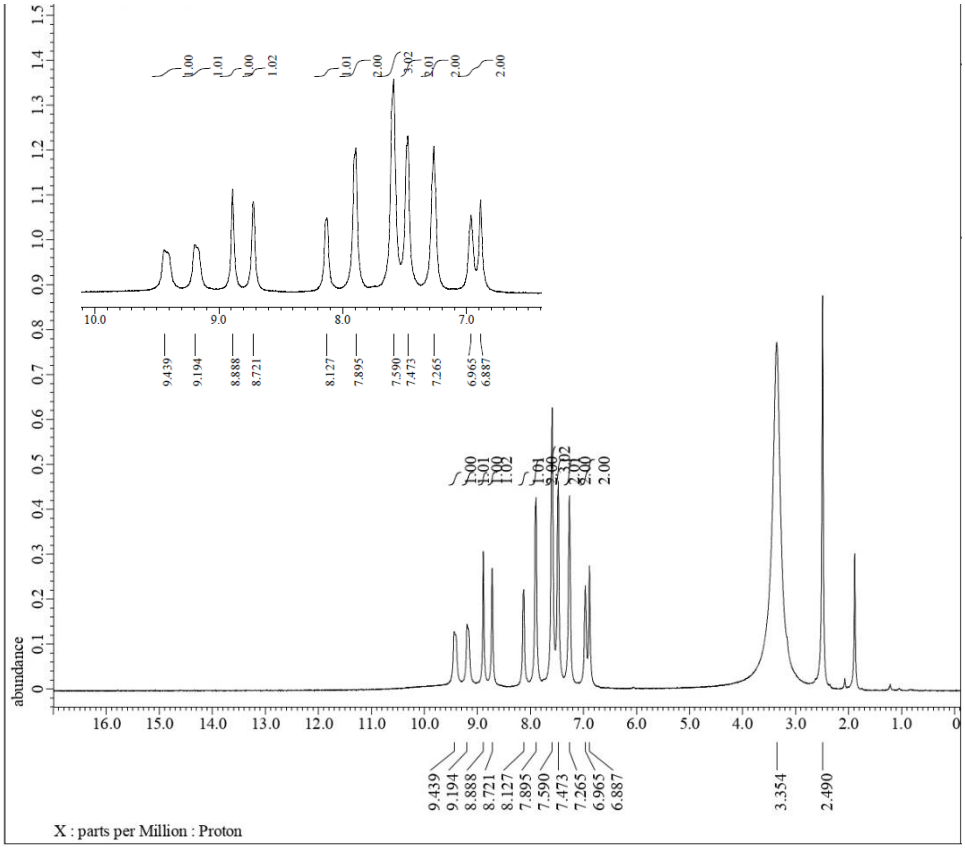

Figure S41. ^{1}H NMR (500 MHz, DMSO-d_6) spectrum of compound **2m**

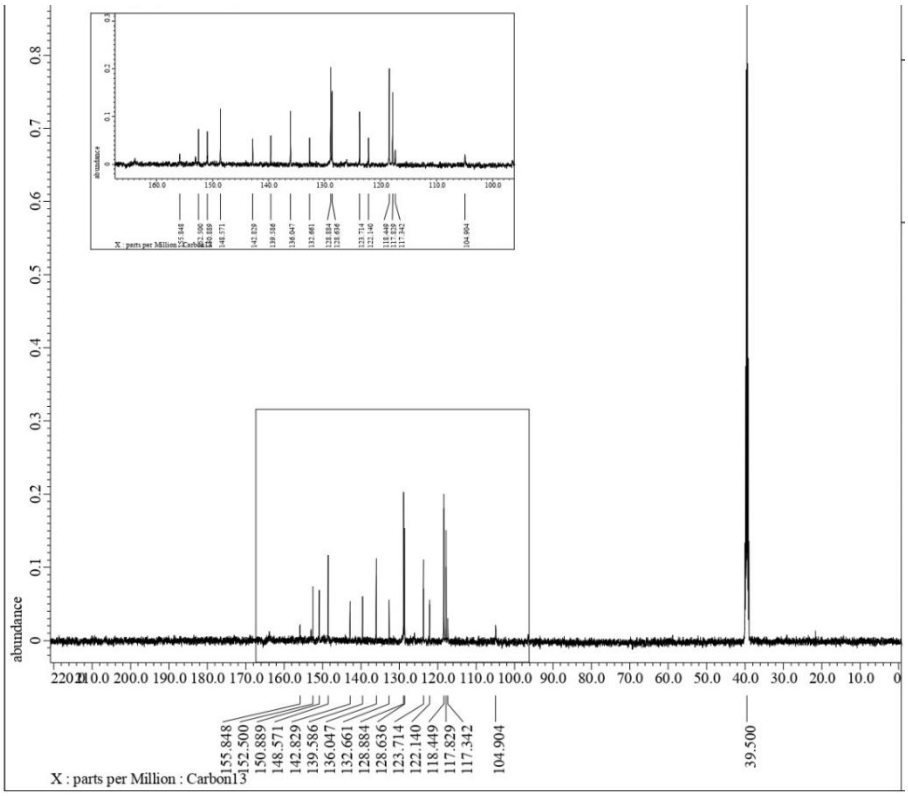

Figure S42. ^{13}C NMR (125 MHz, DMSO-d_6) spectrum of compound **2m**

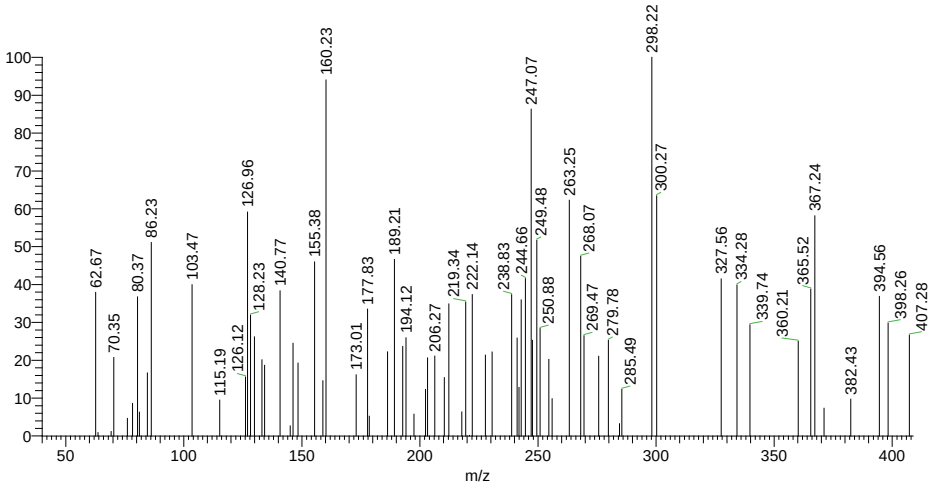

Figure S43. Mass spectrum of compound **2m**

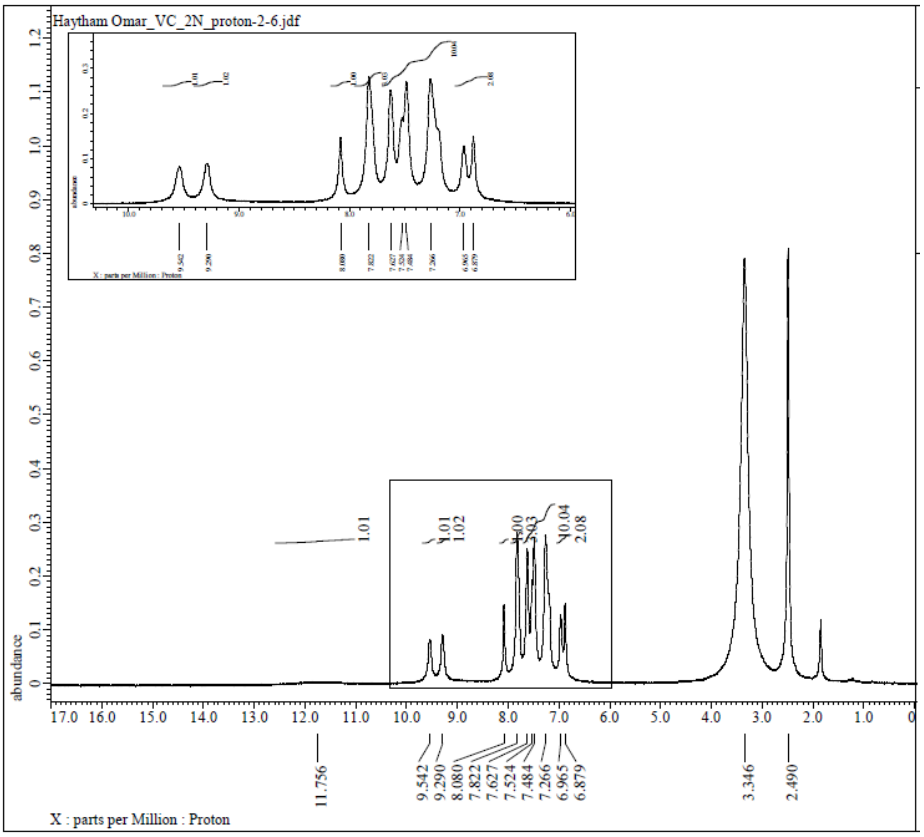

Figure S44. ^{1}H NMR (500 MHz, DMSO-d_6) spectrum of compound **2n**

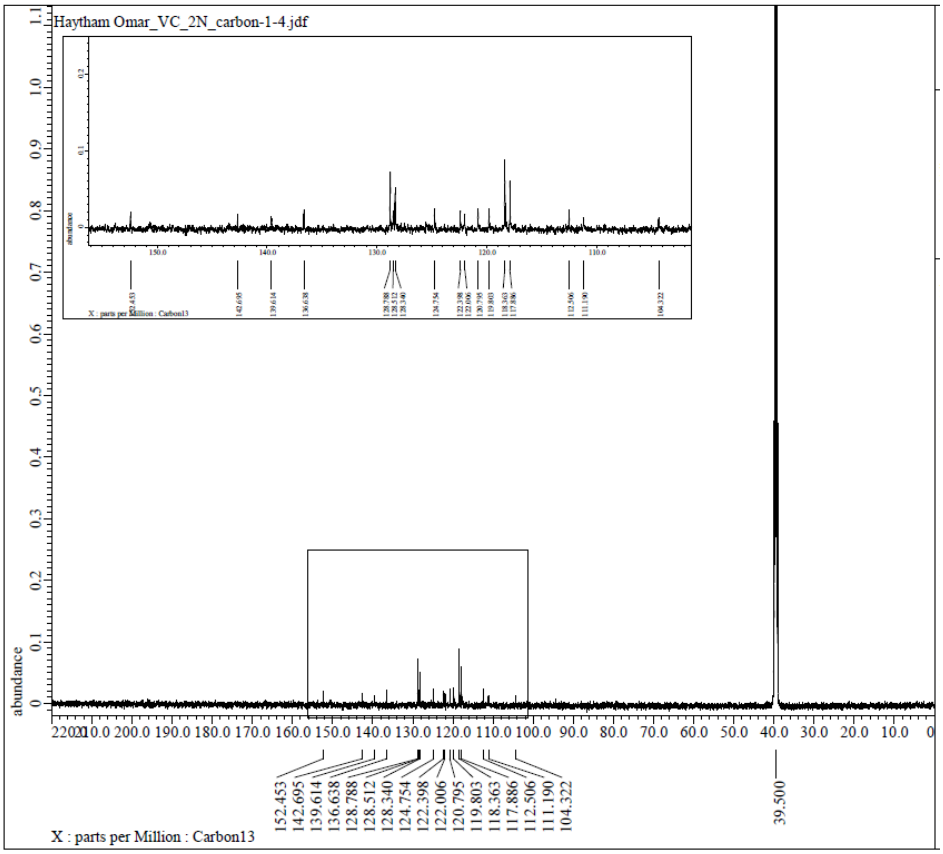

Figure S45. ^{13}C NMR (125 MHz, DMSO-d_6) spectrum of compound **2n**

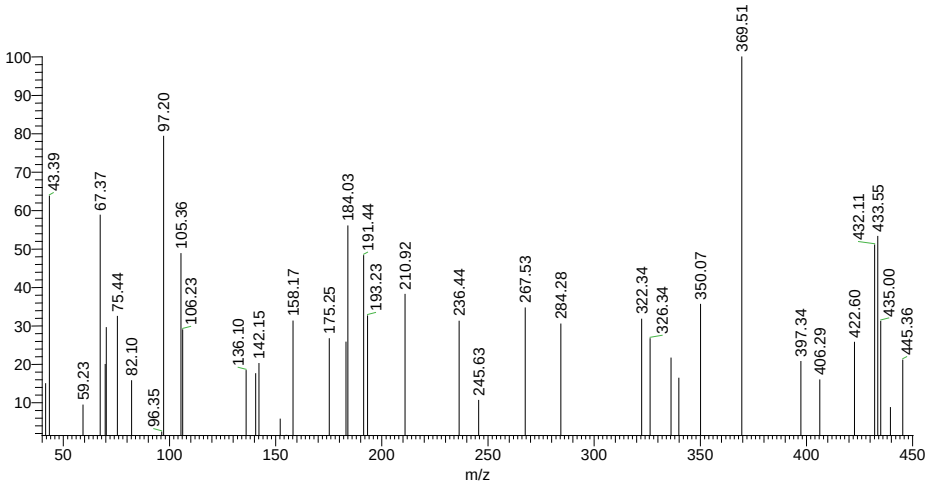

Figure S46. Mass spectrum of compound **2n**

Requester Data

Name:	**Haytham O. Tawfik**	Tel.	**01005356819**
Authority:	**Faculty of Pharmacy Tanta University**	Date	**30/03/2023**

Sample Data

Samples had been submitted for elemental analysis.

Analysis Report

No.	Code	C%	H%	N%
1	**2a**	73.60	4.50	13.66
2	**2b**	68.38	4.01	12.59
3	**2c**	62.11	3.44	11.44
4	**2d**	73.95	4.91	13.45
5	**2e**	71.33	4.50	12.77
6	**2f**	66.69	3.75	15.64
7	**2g**	63.01	3.49	11.87
8	**2h**	63.00	3.33	11.70
9	**2i**	62.98	3.45	11.80
10	**2j**	52.01	2.91	9.54
11	**2k**	67.99	4.99	11.35
12	**2l**	76.54	4.52	12.40
13	**2m**	70.98	4.25	17.25
14	**2n**	72.52	4.18	15.85

INVESTIGATOR **DIRECTOR**

Figure S47. Elemental analysis of compounds **2a-n**

HPLC Protocol Data

The lead compounds were tested for purity using HPLC (Agilent™ 1260 Infinity HPLC system equipped with Agilent 1260 Infinity quaternary pump (G1311C), Agilent 1260 Infinity thermostated column compartment (G13b16A), Agilent 1260 Infinity autosampler with reliable injections from 0.1 to 100 µL (G1329B) and Agilent 1260 Infinity UV detector (G1321C). Data was recorded and analyzed with Agilent OpenLAB CDS ChemStation Edition software. HANNA pH 211 Microprocessor pH meter with double junction glass electrode was used to adjust the pH. The column used in HPLC was ZORBAX Eclipse plus C18 (250 x 4.6 mm, 3.5µm). Mobile phase consisted of Acetonitrile (ACN)/0.05M KH_2PO_4 buffer pH3.7 (30:70), flow rate of 1.5 mL/min and the run time was set as double the elution time of each compound. Their purity was recorded with a high percentage (≥95).

```
================================================================================
Acq. Operator   : SYSTEM
Sample Operator : SYSTEM
Acq. Instrument : HPLC                              Location : Vial 15
Injection Date  : 8/23/2023 1:28:39 PM
                                                  Inj Volume : 5.000 µl
Method          : C:\CHEM32\1\METHODS\DEF_LC.MCYANO COLUMN.M
Last changed    : 8/23/2023 2:39:15 PM by SYSTEM
                  (modified after loading)
Sample Info     : 30 ACN:70 phosphate buffer pH 3.7, Flow 1.50 mL/min, 254 nm, 5 ul injection
```

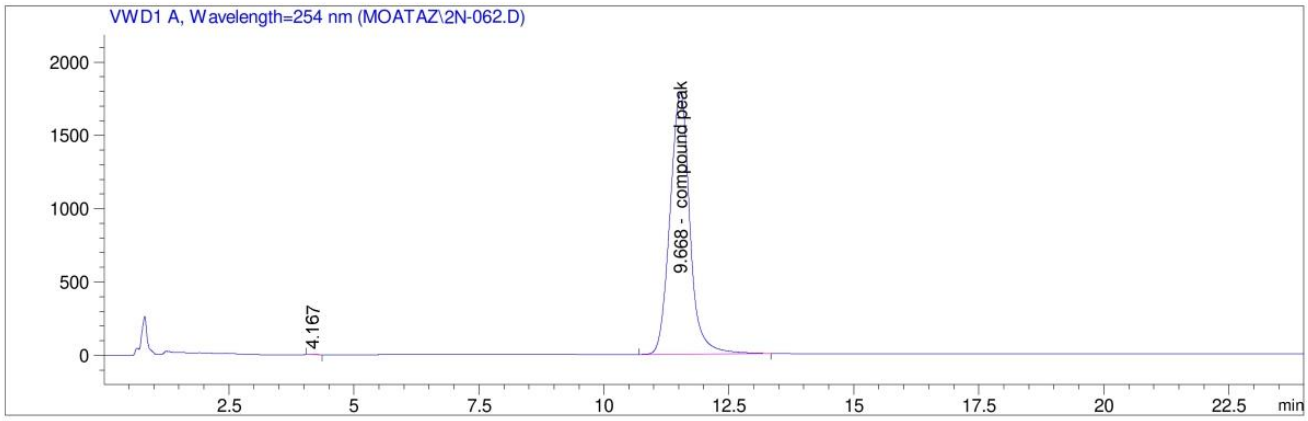


```
================================================================================
                          Area Percent Report
================================================================================

Sorted By             :      Signal
Calib. Data Modified  :     8/23/2023 2:39:15 PM
Multiplier            :      1.0000
Dilution              :      1.0000
Sample Amount:                :   0.50000     [mg/ml]   (not used in calc.)
Do not use Multiplier & Dilution Factor with ISTDs

Signal 1: VWD1 A, Wavelength=254 nm

Peak RetTime  Type   Width     Area      Area    Name
  #   [min]          [min]   [mAU*s]       %
----|-------|------|-------|----------|--------|---------------------
   1   9.668         0.3852  2.06465e4  98.5384 compound peak


Totals :                     2.06465e4  98.5384

                         *** End of Report ***
```

Figure S48. HPLC chart of compound **2n**

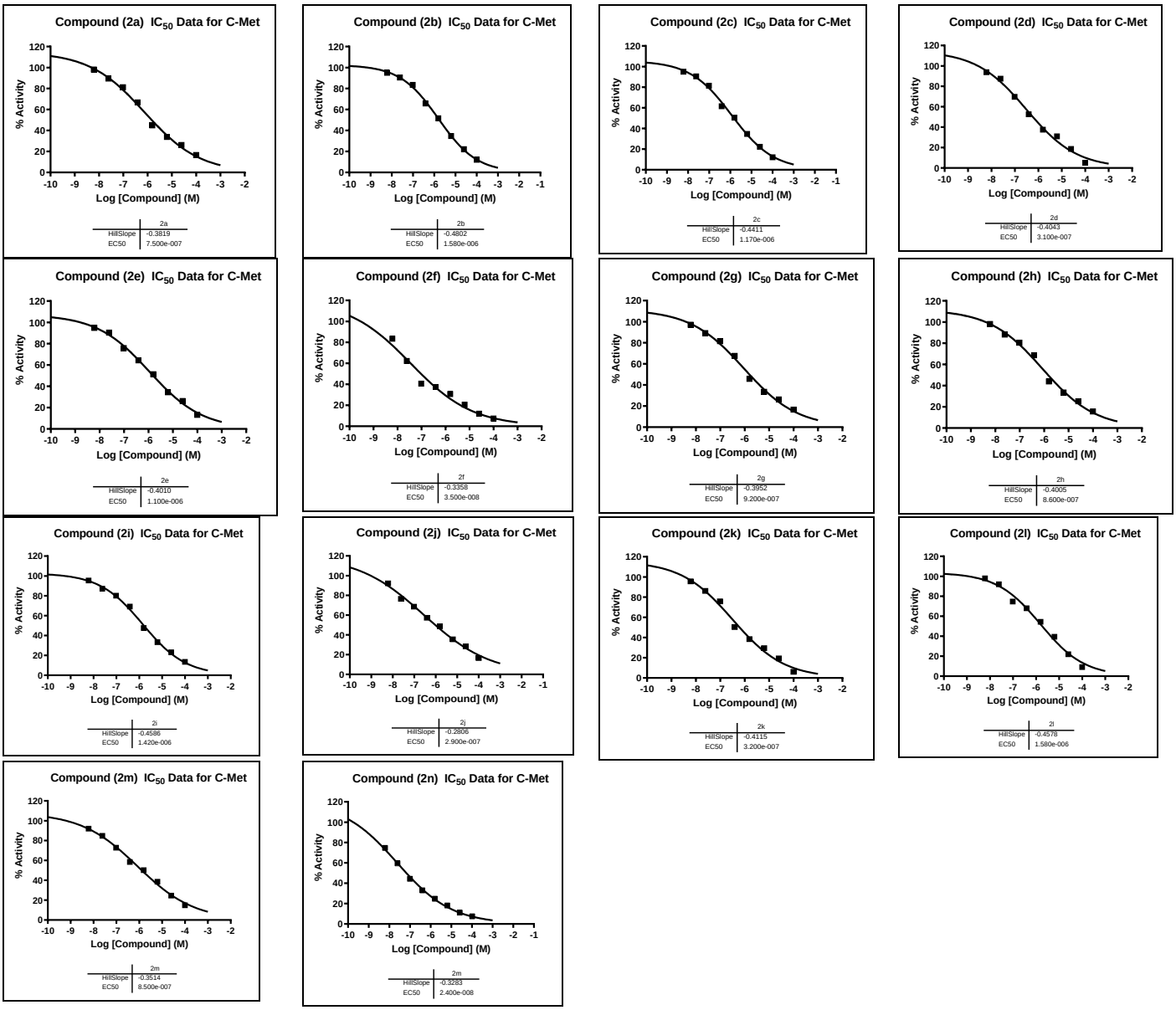

Figure S49. Inhibition ratio curves of **2a-n** towards c-Met. Different compound concentrations were set in the assay.

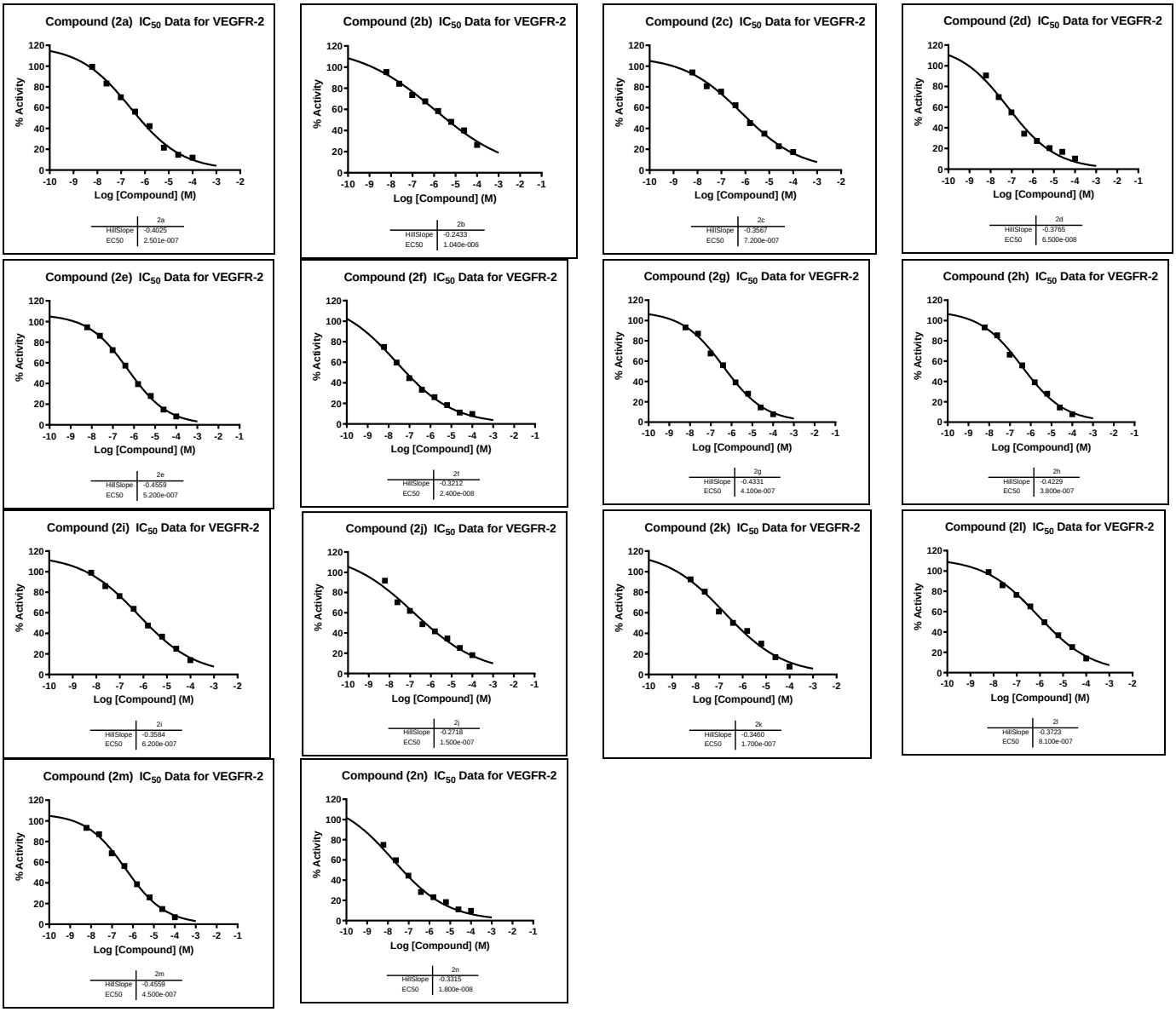

Figure S50. Inhibition ratio curves of **2a-n** towards VEGFR-2. Different compound concentrations were set in the assay.

Table S1. Percent kinase activity and inhibitory values of compound **2n** against a panel of kinases

Kinase	Kinase activity (%)	Kinase inhibitory activity (%)
p38a MAPK	98	2
SGK1	93	7
GSK3b	104	-4
Aurora B	103	-3
MARK3	85	15
Src	89	11
BTK	97	3

Biology Protocols

c-MET and VEGFR-2 kinase inhibition Assays

All molecules were evaluated for their c-MET (BPS Bioscience Corporation catalog #79559) and VEGFR-2 kinase inhibition using (BPS Bioscience Corporation catalog#40325) using ELISA kit (Enzyme-Linked Immunosorbent Assay). They were solvated in DMSO (0.1%), and serial diluations (four conc.) were set following the manufacturer's instructions.

Cytotoxicity

Both breast cancer "MCF-7" and prostate cancer "PC-3" and normal "WISH" cells were purchased from the National Research Institute, Egypt, and maintained in RPMI-1640 medium L-Glutamine (Lonza Verviers SPRL, Belgium, cat#12-604F). All cells were incubated at 37 ºC in a 5% carbon dioxide atmosphere (NuAire). Cells were plated at a density of $5x10^4$ cells in triplicates in a plate of 96 wells. On the second day, cells were treated with the compounds with concentrations of (6.25, 12, 25, 50, and 100 µM). Cell viability was assessed using the MTT assay.

Investigation of apoptosis

Annexin V/PI staining and cell cycle analysis

MCF-7 cells were seeded into 6-well culture plates (3-5× 10^5 cells/well) and incubated overnight. Cells were treated with compound **APPU 2n** at their IC_{50} values for 48 h. Next, media supernatants and cells were collected and rinsed with ice-cold PBS. Then, cells were suspended the cells in 100 µL of annexin binding buffer solution "25 mM $CaCl_2$, 1.4 M NaCl, and 0.1 M Hepes/NaOH, pH 7.4" and incubated with "Annexin V-FITC solution (1:100) and propidium iodide (PI)" at a concentration equals 10 µg/mL in the dark for 30 min. Stained cells were then acquired by BD FACSCalibur™ Flow Cytometer.

Real-time-polymerase chain reaction for the selected genes

Gene expression of Bcl-2, the anti-apoptotic gene, and the pro-apoptotic genes "P53, Bax, and Caspapses-3,8, and 9" were examined to delve deeper into the apoptotic pathway. MCF-7 cells were then treated with compound **APPU 2n** at their IC_{50} values for 48 h. After treatment, the RT-PCR reaction was carried out following routine

work. Then, the Ct values were collected to calculate the relative genes' expression in all samples by normalization to the β-actin housekeeping gene.

***In Vivo* Assay**

Animals and tumor cell line

Adult female Swiss albino mice purchased from Theodor Bilharzia Research Institute, Giza, Egypt, with an average body weight of (18-23) g was used. Mice were housed under constant conditions of 12 h light/dark cycle in a temperature under conditions of controlled humidity (22 ± 2 °C), with free access to standard laboratory mice food and water.

Solid Ehrlich carcinoma (SEC) cells were got from the National Cancer Institute (Cairo University, Egypt). The tumor cell line was proliferated in mice through serial intraperitoneal (I.P.) transplantation of a volume of 0.2 mL physiological saline containing 1×10^6 viable cells for 24 h. SEC cells were collected 7 days after I.P. implantation. The harvested cells were diluted with saline to obtain a concentration of 5×10^6 viable SEC cells/mL. A volume of 0.2 mL saline contains 1×10^6 SEC cells that were I.P. implanted into each normal mouse. SEC cells (1×10^6 tumor cells/mouse) were implanted subcutaneously into the right thigh of the hind limb.

The experimental animals were randomly divided into four groups. Group 1 served as the normal saline control. Group 2 served as the SEC control (1×10^6 cells/mouse). Group 3 served as the compound **2n**-treated group (6 mg/kg B.Wt., I.P.). Group 4 received the standard anticancer drug of Cabozantinib (6 mg/kg BW, I.P.) and is considered as a reference control. Body weight and survival were recorded daily until the 24th day in both treated and control groups. At the end of experiment, the blood of each group was collected under light anesthesia for estimation of hematological assays. The anesthetized animals were then sacrificed for evaluation of the antitumor activity examination.

Antitumor potentiality

It includes tumor volume, weight, and tumor inhibition ratio (TIR%). Time interval measurements of tumor volume using digital Vernier caliper (Tricle Brand, Shanghai, China). Measure tumor length and width using clipper and then calculate tumor volume using formulations V = (L x W x W)/2, where V is tumor volume, W is tumor width, L is tumor length. While TIR% was calculated according to the following equation $\frac{Tumor\ volume\ (Control) - Tumor\ volume\ (treated)}{Tumor\ volume\ (control)} x\ 100$.

Blood assays

At the end of the experiment, animals from different groups were sacrificed, and blood samples were collected for determination of was estimated using Abbott CELL-DYN® 1800 automated hematology analyzer (USA) with ready-made kits (Abbott Laboratories, Abbott Park, IL, USA).

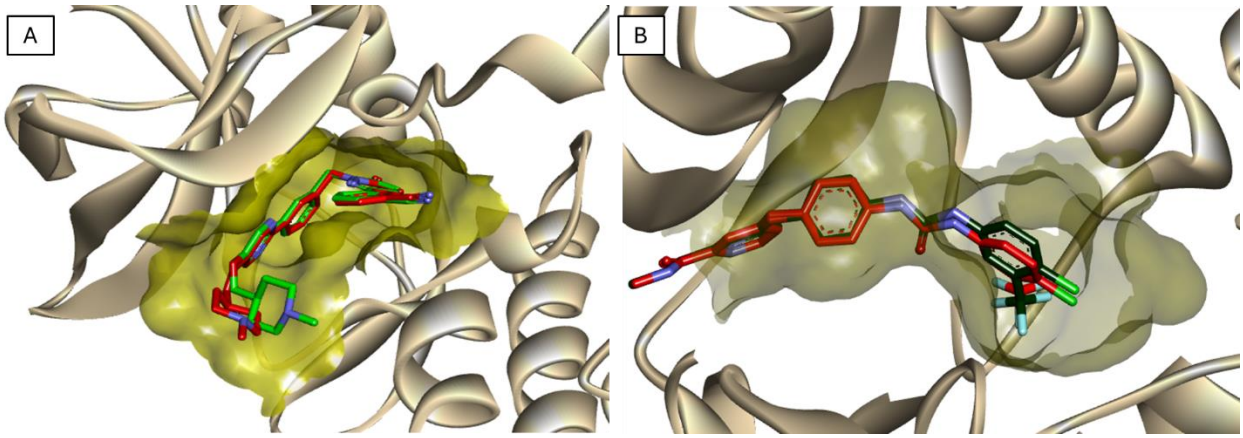

Figure S51. Overlay of the docked ligand (green) with the co-crystalized ligand (red) inside the active site of A) c-MET (RMSD= 1.0906 Å) and B) VEGFR-2 (RMSD= 1.0042 Å) receptors.

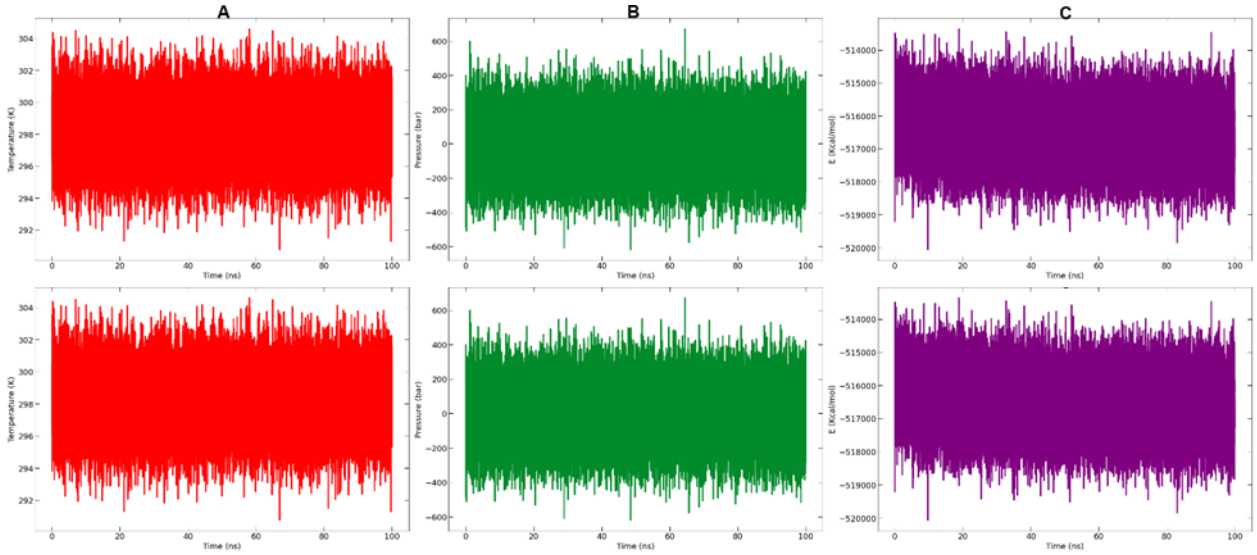

Figure S52. From left to right: **(A)** Temperature, **(B)** pressure and **(C)** potential energy during the 100ns MD simulations (Top: VEGFR-2 system and Bottom: c-MET system).

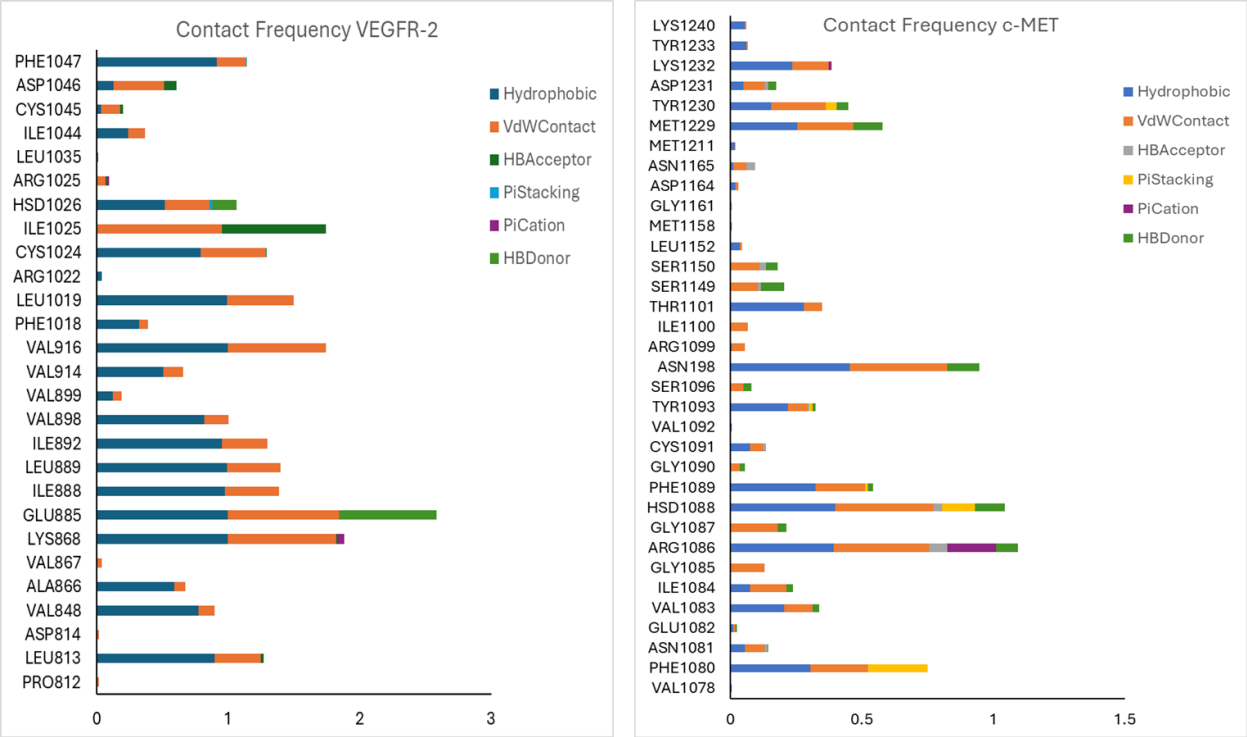

Figure S53. Frequency of interacting residues and type of interaction for **2n** with VEGFR-2 and c-MET receptors.